EVALUATION OF A THIOL-MODIFIED HYALURONAN AND ELASTIN-LIKE POLYPEPTIDE HYDROGEL FOR NUCLEUS PULPOSUS TISSUE ENGINEERING

by

Diana Lee

A thesis submitted to the Department of Chemical Engineering

In conformity with the requirements for

the degree of Master of Applied Science

Queen's University

Kingston, Ontario, Canada

(March, 2011)

Abstract

Degenerative disc disease (DDD) is a common medical issue among human adults, leading to back pain and potentially, disability, decreasing an individual's quality of life. In the United States alone, huge economic impacts are apparent with an estimated $50-100 billion attributed to lost productivity and medical costs related to DDD. Spinal degeneration occurs in the intervertebral disc (IVD) and once damaged, the IVD is incapable of adequate self-repair. A regenerative therapy incorporating nucleus pulposus (NP) tissue engineering may provide an answer to spinal degeneration. The objective of this *in vitro* study was to evaluate the potential of a thiol-modified hyaluronan (TMHA) and elastin-like polypeptide (ELP) as a hydrogel scaffold for nucleus pulposus tissue engineering. Two materials, one composed of TMHA only and one a 3:1 TMHA/ELP, crosslinked with polyethylene glycol diacrylate (PEGDA), were seeded with cultured human NP cells and cyclic hydrostatic loading was applied at 1MPa for 3 hours a day for 3 consecutive days. Cell viability and gene expression were analyzed. A decreasing trend in cell viability with time and cyclic hydrostatic pressure loading was observed and statistically significant differences were observed between the TMHA unloaded treatment group at day 0 and the TMHA loaded treatment group at day 4 and between the TMHA unloaded treatment group at day 0 and the 3:1 TMHA/ELP loaded group at day 4. Comparisons between TMHA only and 3:1 TMHA/ELP hydrogels for the same treatment indicate similar trends and no statistically significant differences in biological effects were observed. Gene expression analysis indicated low frequency expression of NP extracellular matrix (ECM) molecules regardless of time point or cyclic hydrostatic

pressure application. These results are revealing in that the 3:1 TMHA/ELP hydrogel did not support NP cells significantly better than the TMHA hydrogel, though cell source and hydrostatic pressure generation issues may have impacted this finding. Additional studies with alternative cell type and a refined hydrostatic pressure application method may better illuminate the efficacy of a 3:1 TMHA/ELP hydrogel as for NP tissue engineering.

Acknowledgements

I would like to thank my supervisor Dean Kimberly Woodhouse for providing continuous guidance, support and encouragement throughout the course of this research. It has been quite an experience and I have learned a lot, not only about research but also about life.

Thank you to my committee members, Dr. Cari Whyne and Dr. Brian Amsden for taking the time to critique this work and offer insight. Thank you to Dr. Margarete Akens for all of your help and advice with the experiments and flow cytometry and to Dr. Albert Yee for providing me with disc samples for this research. Thank you to Jessica Rouleau for providing me with ELP and Dr. Chris Hrabchak for all the PCR assistance.

Thank you to the OBL members, particularly Ashley Leckie and Rachel Keshwah, for your friendship throughout the course of this project.

To my family and friends, thank you for all of your understanding and support through the all the highs and the lows.

I would like to dedicate this thesis to Katie McAlindon. From biology undergrad to chemical engineering graduate studies you provided your friendship, understanding and support along the way. You were my partner in crime from the beginning of this journey and I will always remember our experiences in the Yukon and Northwest Territories and all of our antics and inside jokes, you are greatly missed.

Table of Contents

List of Figures

List of Tables

Glossary

AF	annulus fibrosis
DDD	degenerative disc disease
DMEM	Dulbecco's Modified Eagle's Medium
ECM	extracellular matrix
EDTA	ethylene diamine tetraacetic acid
ELP	elastin-like polypeptide
FBS	fetal bovine serum
GAG	glycosaminoglycan
HA	hyaluronan
IVD	intervertebral disc
LBP	low back pain
MSC	mesenchymal stem cells
NP	nucleus pulposus
NPR	nucleus pulposus replacement
PBS	phosphate buffered saline
PCR	polymerase chain reaction
PEGDA	polyethylene glycol diacylate
PG	proteoglycan
P/S	penicillin/streptomycin
RT	reverse transcriptase
TDR	total disc replacement
TMHA	thiol-modified hyaluronan
UHMWPE	ultra high molecular weight polyethylene

Chapter 1 Introduction

1.1 Motivation

The majority of individuals will experience mechanical low back pain (LBP) at some point during their lives [1]. Though there is contention regarding the exact etiology, LBP is widely believed to result from the degeneration of the intervertebral disc (IVD). This degeneration can result in back pain, disability and a decreased quality of life. It is commonly thought that the degenerative cascade begins in the nucleus pulposus (NP), the core of the intervertebral disc, where an imbalance in the production and degradation of the IVD extracellular matrix (ECM) components contribute to the structural and functional deterioration of the IVD [2]. Once damaged, the disc is incapable of adequate self-repair, with no restoration to its original form and function. LBP has a lifetime prevalence of 60-80% [3] and is attributed to an estimated $50-100 billion in lost productivity and medical costs in the United States alone [4]. In Canada, LBP recurrence rate was observed in a group of over 2000 individuals who were unable to work for a time period of 6 months or more due to chronic back pain. In the 1-year follow-up, 20% of those surveyed had recurring issues with LBP and in the 3-year follow-up 36% of those surveyed indicated recurring LBP issues [5, 6]. Rossignol and others conducted a study following 2300 individuals in Quebec, Canada who experienced LBP and found that 6 months after the initial survey, 6.7% of the sample population was still absent from work, which amounted to 68% of lost work days and 76% of total LBP compensation cost [6].

Current treatments target end-stage DDD and are typically limited in their ability to offer long-term solutions and recurring problems in the same or adjacent discs are common. A regenerative therapy encompassing tissue engineering strategies may provide an answer to spinal degeneration where disc repair and long-term sustainability are involved, specifically, through the application of minimally invasive strategies that may halt or reverse symptomatic degeneration. As such, NP tissue engineering may offer an attractive option for the treatment of early state degenerative disc disease (DDD).

1.2 Project Objective

The main objective of this project is to evaluate, *in vitro,* the potential of a TMHA and ELP composite hydrogel as a potential scaffold for intervention of early-stage IVD degeneration.

The specific objectives of the project are:

1) To apply dynamic (cyclic hydrostatic pressure) loading conditions to TMHA and ELP nucleus pulposus cell-seeded scaffolds
2) To evaluate cell morphology and viability in TMHA and ELP nucleus pulposus cell-seeded scaffolds prior to and following cyclic hydrostatic pressure
3) To evaluate gene expression in TMHA and ELP nucleus pulposus cell-seeded scaffolds to observe the effect, if any, of cyclic hydrostatic pressure application

Chapter 2 Literature Review

2.1 Spine Anatomy

The human spine is a composed of four main sections: cervical, thoracic, lumbar and fused vertebrae and includes 7 cervical, 12 thoracic, 5 lumbar, 5 sacral and 4 coccygeal vertebrae, one stacked atop the other. The spine is the main component of the axial skeleton [7].

The mechanical structure serves three main functions: transfer of force and moments of the head, trunk and pelvis, physiological motion between body parts, and protection of the spinal cord. The shape of the spine is curvilinear with four curves in the saggital plane to increase column flexibility and provide shock-absorption while retaining sufficient structural support and stability. Ligaments and discs interconnect the vertebrae.

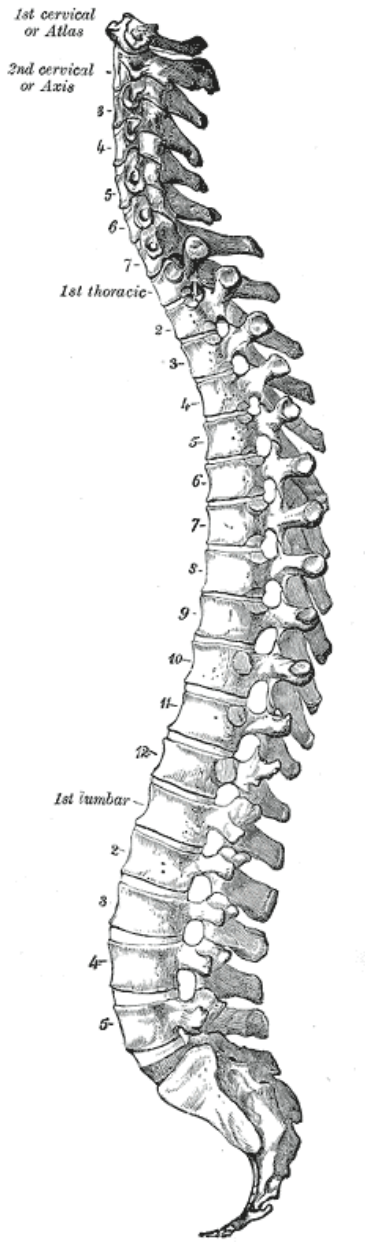

Figure 2-1. Lateral view of the vertebral column [7]
Image from Gray's Anatomy, copyright expired.

The vertebral foramen consists of the body and disc [8]. The vertebral body is the main load-bearing component of the spine and the vertebral bodies articulate vertically with each other via facet joints. The IVDs lie between adjacent spinal vertebrae and acts as fibrocartilaginous 'cushions,' allowing for shock absorption..

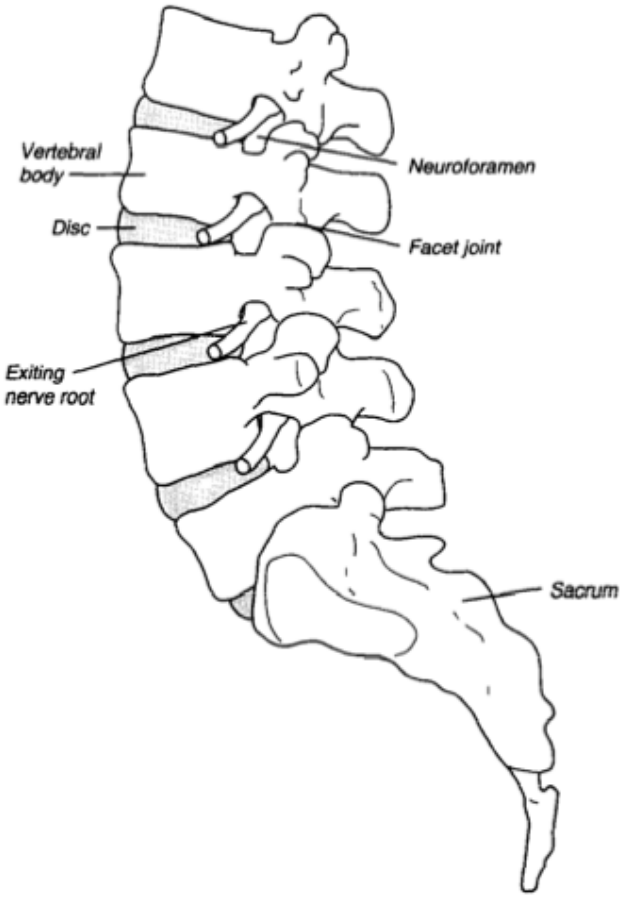

Figure 2-2. Anatomy of the lumbar spine [9].
Image used with permission: Elsevier Limited, copyright 1996.

2.2 Intervertebral Disc

The annulus fibrosus (AF), nucleus pulposus (NP), and cartilaginous end-plates constitute each IVD. The AF is elastic and consists of concentric sheets of collagen fibres orientated at distinct angles, enclosing the NP. This outer fibrocartilaginous cortex of lamella, layered in alternating orientations, provides strength while allowing movement. Superior and inferior to the disc, thin hyaline cartilage endplates cap the gelatinous and proteoglycan-rich NP located the centre of the IVD. As the discs are

avascular, these endplates also diffuse nutrients from peripheral and adjacent blood vessels [10].

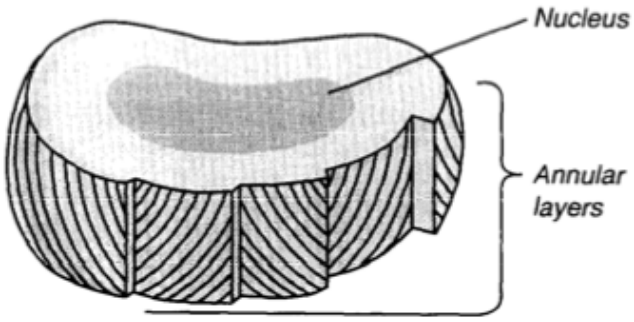

Figure 2-3. Structure of an intervertebral disc [9].
Image used with permission: Elsevier Limited, copyright 1996.

The difference in tissue composition between the NP and the AF can be attributed to their origins. During embryonic development, the NP is formed from the notochord whereas the AF is formed from mesenchymal tissue [11]. The notochordal cells are responsible for producing large aggregate proteoglycans (PG), inducing an environment rich in PGs. The notochordal cells are eventually replaced by chondrocyte-like cells and generate an extracelluar matrix (ECM) containing PG and collagen [1]. Aggrecan, a PG in the nucleus pulposus is a negatively charged molecule composed of sulphated glycosaminoglycan (GAG) sidechains, chondroitin and keratin sulphate. Aggrecan, along with hyaluronan (a nonsulphated GAG), form aggregate molecules and thereby attract water, contributing heavily to the NP mass. The ECM of the NP also contains collagen, predominantly type II, and elastin. The type II collagen imparts strength, compressive ability and resistance to deformations while the elastic fibres allows for

structural support and elastic recoil. The AF is abundant in collagen type I, and serves as a fibrocartilage structure enclosing the NP. The concentric arrangement of lamellae that make up the AF offers tensile strength, flexibility and the ability to withstand shear loads [12].

Cells of the NP are observed to be large, round and chondrocyte-like and mainly express collagen type II and aggrecan in the ECM [13]. The outer AF cells are fibroblast-like and have a long and thin form and predominantly express collagen type I.

NP cell phenotype is characterized as an ECM rich in aggrecan and collagen type II. Three distinct phases have been observed in ECM turnover of the IVD [14]. In phase I, the growth period, active synthesis of ECM molecules are observed with active denaturation of collagen type II [14]. Phase II, maturation and aging, is distinguished by a decrease in synthesis and a reduction in collagen type II denaturation but with an increase in procollagen type I [14]. During the degenerative third phase, a lack of aggrecan and procollagen type II is observed coupled with an increase in collagen type II denaturation and procollagen type I synthesis [14]. This result suggests a correlation between collagen type II degeneration with age and an increase in collagen type I synthesis with age in the IVD [15].

Two genes relevant to the NP are CD24 and SOX9. CD24 is an anchor protein and a molecular marker for the NP [16]. Findings demonstrate a high level CD24 of gene expression in the NP with CD24 expression apparent in herniated NP tissue [16]. SOX9

is an essential transcription factor for collagen type II synthesis and for chondrogenesis [17]. It is an important driver of the NP cell phenotype and plays a major role in differentiation and maintenance of the chondrocytic phenotype.

2.3 Cyclic Hydrostatic Loading

In vivo, tissues and cells undergo mechanical stimulation and this applied pressure plays a role in the tissue repair process [18]. Normal IVD cells are exposed to a variety of mechanical stresses due to the muscle forces and ligament tensions associated with posture and movement in daily activities. From these mechanical stresses, the IVD cells are subject to cyclic loading and unloading and this stimulation is vital for normal disc cell function though a fine balance exists between pressure resulting in anabolic effects and pressure resulting in catabolic effects [19]. Angele and others have demonstrated the positive effects of hydrostatic loading on cartilaginous matrix formation of mesenchymal progenitor cells, insinuating the significance of mechanical force in cartilage repair and regeneration [20]. In another study, when chondrocytic cells were subject to a range of intermittent hydrostatic pressure *in vitro*, an increase in ECM production was observed [21, 22].

2.4 Degenerative Disc Disease

The exact definition of degenerative disc disease is still under contention, where some group degeneration and aging together and others believe DDD is an entirely separate process. As well, there are no clear criteria to distinguish between disc degeneration as a result of aging and disc degeneration occurring from a pathologic

process [11]. Despite the uncertainty surrounding the exact definition and cause of disc degeneration, it is commonly believed that the degenerative cascade originates in the nucleus pulposus [12]. Degenerative disc disease disturbs the mechanical balance between the central gel-like nucleus pulposus and the surrounding lamellar annulus fibrosus through gradual loss of water, proteoglycans and collagen [23]. In a healthy intervertebral disc, the water content in the nucleus pulposus acts as an incompressible cushion, allowing for spinal stress absorption. In degenerative disc disease, the nucleus pulposus loses its ability maintain a fluid pressure in the disc, consequently losing its capacity to resist external loads [24].

One of the main factors contributing to disc degeneration is the avascularity of the disc, where diffusion is the sole method for receiving nutrients and removing waste [25]. As the disc matures over time, the centre becomes increasingly isolated from the blood vessels and the endplates become sclerotic and less porous [9]. The decrease in porosity affects oxygen, glucose and amino acid levels and results in a build-up of metabolic waste [10]. The build-up of waste is harmful since the cells of the IVD are in a hypoxic environment and undergo anaerobic oxidation yielding lactic acid. The lactic acid acidifies the ECM and impacts regular cell function, typically inducing apoptosis in any remaining notochordal cells and also a portion of the mesenchymal cells. As cells in the disc advance toward senescence and the already low density of cells continue to decrease in viability, an imbalance becomes apparent between normal matrix molecule synthesis and degradation [2, 10, 12]. The resulting effect changes the biochemical structure and composition of the ECM and collagen type II is denatured and degraded and supplanted

by collagen I fibrils [26]. The avascularity of the disc limits regenerative capability and once damaged, the disc is incapable of adequate self-repair, unable to be restored its original state and function.

Mechanical and genetic factors can also contribute to disc degeneration. Though intermittent compressive loading is beneficial and necessary for normal cell function, such as cell metabolism and PG synthesis, adverse loading can be antagonistic and leave the cells vulnerable to degeneration and herniation [27]. Genetic influences, such as polymorphisms in different individuals may also contribute to the effects of disc degeneration and impact susceptibility and tolerance levels to adverse mechanical loading [2].

2.5 Current Treatment Options

Current treatments for degenerated discs are often geared toward the symptoms of end-stage lumbar spine degeneration and can be invasive. While these treatments offer some clinical relief, there is a limit in their ability to offer long-term solutions. The array of treatments offered tends to focus on drugs, physical therapy and surgeries and though relief may be achieved, it is not uncommon for the treated disc or adjacent discs to become a repeat issue, as the underlying biology of DDD has not been treated.

2.5.1 Discectomy

Discectomy is the most common surgical treatment for relief of low back pain due to disc degeneration. In a discectomy, the offending disc is completely removed. In a nucleotomy, only the protruding NP portion of the IVD is removed. Which type of

surgery is performed is dependent upon the situation, taking into consideration damage to the AF and NP protrusion. Traditional discectomys and nucleotomys involve invasive open surgery of the back including a sizeable incision in the AF. More recent techniques utilize a small cannulae reducing the size and potential damage to the AF.

In a nucleotomy the load-bearing role of the NP is conferred upon the surrounding tissue, often affecting spinal stability and propagating the degeneration cascade on the inflicted level or adjacent discs. When the NP is partially removed, the remaining IVD is not able to withstand applied loads and resist compression. In a full nucleotomy, the surrounding AF tissue often moves inward in the IVD, altering the IVD shape and its functions. The loss of NP material resulting in decreased disc height renders the IVD incapable of its original ability to resist compression, enhancing the effect of degeneration if any NP is remaining and likely resulting in a need for reoperation for the same disc or adjacent discs.

2.5.2 Spinal Fusion

Spinal fusion is another common treatment for DDD. In 2002, approximately 200 000 spinal fusion surgeries were performed in the United States to alleviate pain associated with disc degeneration [28]. In fusion surgery, the entire IVD is removed and a bone graft is inserted and fused between the adjacent vertebrae in an effort to eliminate motion in the offending site caused by a herniated or degenerate disc [9]. The source of the bone graft is typically retrieved from autogenic sources such as the patient's own pelvis, which requires an additional procedure and can lead to post-operative concerns

with infection, nerve or vascular injury abdominal herniation [29]. Allogeneic sources, typically harvested from cadavers have also been utilized. Allogeneic sources offer less limitation with regard to amount of bone available for the fusion however, cells are removed to minimize immunologic responses in the patient, producing a bone graft that is not osteogenic [29]. With no capability to synthesis new bone, the graft may form a stable arthrodesis [29]. Post-operative complications associated with allogeneic bone grafts can include pseudoathrodesis (vertebrae do not fuse together), or fracture after implantation [29].

Regardless of graft source, spinal fusion surgeries have the potential for complications and associated risks, some of which include bone graft site tissue morbidity, graft migration and fusion failure and adjacent segment degeneration (ASD). Additionally, the limit in range of motion and stiffness associated with fusion surgery can have adverse biomechanical effects on the adjacent discs and vertebrae, resulting in further degeneration and back pain [9, 28].

2.5.3 Total Disc Replacement (TDR)

One device utilized for spinal surgery is the Charité disc. This is a total artificial disc device with the intention of replacing the degenerate disc. Developed in the mid-1980s, this disc has the longest and largest study of any existing artificial disc [9]. Though the device has been in operation in Europe for the last 20 years, the SB Charité® disc only obtained FDA approval in 2004 and is currently being marketed in the United States [30]. The disc is composed of a convex polyethylene oval spacing piece

sandwiched between two concave end-plates of cobalt-chromium alloy with spikes to allow fixture to the vertebral body [31].

Figure 2-4. Charité disc, a total disc replacement device [31].
Image used with permission: DePuy Spine Incorporated, copyright 2010.

The polyethylene used in the Charité disc is an ultra high molecular weight polyethylene. The most notable properties of ultra high molecular weight polyethylene are its chemical inertness, lubricity, impact resistance and abrasion resistance, making it a popular material for orthopaedics devices. The Charité disc is made from a non-polar and hydrophobic material, which can make bonding to other polymers, and tissue, difficult and it is a non-biodegradable material [32]. Toxicity issues resulting from debris wear and foreign body reactions can be of a concern. In a study by van Ooji and others, the presence of polyethylene was found in periprosthetic tissue in patients after 6.5 to 12.9 years after implantation [33]. Osteolysis was observed as a result of high release of wear particles over time, suggesting that wear debris release from the implantation of the Charité disc is an important long-term clinical failure mode of total disc artroplasty [33].

2.5.4 Nucleus Pulposus Replacement

Nucleus pulposus replacement (NPR) surgeries have also been assessed in the treatment of early-state degenerative disc disease. This is a less invasive procedure compared to total disc replacement though the procedure, which is a more recent development, has not been as well studied. Nachemson and others developed the concept of nucleus replacement in the early 1960s when they injected a self-curling silicone into the disc space in human cadavers [34]. It was not until 1996, when a middle-aged man was with implanted with PDN®, an experimental prosthetic disc-nucleus device, with the intended purpose of restoring disc function [35]. By 2002, over 550 patients had been implanted with this device [36].

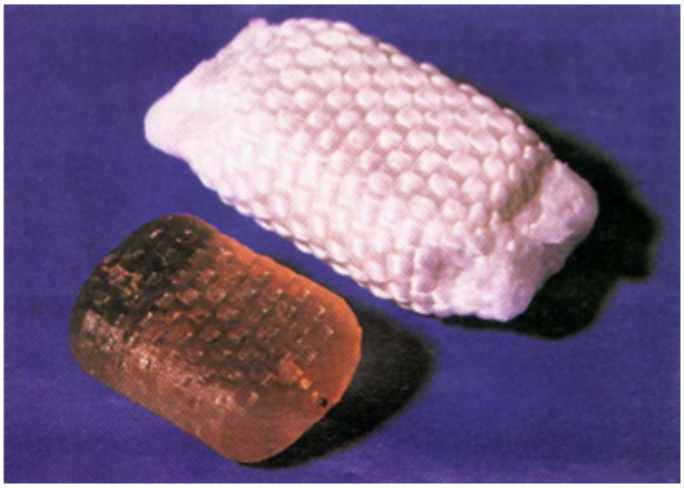

Figure 2-5. Prosthetic disc nucleus, an implantable nucleus pulposus replacement device [28].

The PDN® mimics the cushioning function of the natural nucleus pulposus, maintaining disc height and flexibility. It is composed of a hydrogel pellet of a

copolymer of polyacrylonitrile and polyacrylamide, and encased in a polyethylene jacket. The hydrogel has the ability to absorb 80% of its weight in water, allowing for significant swelling that can restore or maintain disc height [36]. As a control to limit swelling, the high molecular weight linear polyethylene fibres act as a very strong constraining jacket [36] and also functions to minimize horizontal spreading, preserve implant shape, and uphold disc height under spinal loading [37]. Both the hydrogel and polyethylene jacket have undergone mechanical and biological tests simulating typical loading of the spine as well as with burst tests with up to 6000N applied with no detrimental effects [36]. Biocompatibility has also been assessed through systemic toxicity, genotoxicity and carcinogenicity studies and has shown no negative effects [36]. Polyethylene wear debris studies have also been performed and have consistently shown no wear debris production for the device as well [36]. Though acrylamide is a neurotoxin, there does not seem to be any evidence of chemical toxicity from polyacrylamide use though this issue may still be of concern. While early clinical results were encouraging, the implant was not without its complications. Among the concern was implant migration requiring reoperation [38]. Other nucleus pulposus replacement devices, such as the Aquarelle and Newcleus Spiral Implant, are no longer evaluated clinically due to adverse preclinical events [39]. A revised version of the PDN, along with other nucleus replacement technologies, is in various stages of development and remains investigational [39].

While spinal surgery has shown some clinical success [40, 41], fusion, TDR and NPR surgeries are still costly invasive treatments with high risk factors and lengthy recovery times. The underlying pathology is not targeted and issue of adjacent segment

degeneration is a concern. As the degeneration of the spine has high lifetime prevalence, future treatments should look towards procedures that are able to restore not only natural form but function as well. Tissue engineering may provide an answer to degenerative disc disease.

2.6 Tissue Engineering

With huge economic impacts and complications associated with spinal surgery, the future of treating early-stage degenerative disc disease may lie in tissue engineering.

One approach for the treatment of early-stage degenerative disc disease focuses on a regenerative therapy incorporating tissue engineering to target the nucleus pulposus in the intervertebral disc. Current research in the field of tissue engineering utilizes biomaterials to mimic the characteristics of a healthy NP in order to provide structural stability and the means to bear compressive loads while supporting cells and encouraging cell viability and proliferation.

The scaffold is intended to emulate the extracellular matrix and create an environment promoting cell growth and synthesis of new and functional tissue [42, 43]. The scaffold can also be employed as a delivery vehicle for the cells or soluble factors to be implanted at an intended site.

For NP tissue engineering, a 3D scaffold is necessary. The surface should allow cell adhesion, encourage cell growth and proliferation and allow the retention of

differentiated cell function [44]. Biocompatibility is another factor and the scaffold should support regular cell function to optimize tissue regeneration without creating any undesirable responses in the host and any degradation by-products should also be devoid of any adverse systemic effects such as mutagenicity, genotoxicity and carcinogenicity [45]. Porosity should be high to allow sufficient space for cell adhesion, extracellular matrix regeneration and to minimize diffusional constraints [46]. The geometry should support even cell distribution to ensure homogenous tissue formation and the scaffold must also be mechanically strong, to withstand compressive and torsional loading [46]. Another important scaffold consideration is reproducibility and easy fabrication for clinical application [46].

Pre-formed and injectable scaffolds are both options for NP tissue engineering. Pre-fabricated scaffolds are fully formed prior to being seeded with cells and inserted into the NP. With injectable scaffolds, such as hydrogels, cells can be mixed into the scaffold *in vitro* before injection and curing *in situ*. For NP tissue engineering, injectable scaffolds are an attractive option as the insertion procedure is less complicated and less invasive than traditional NP replacement surgeries and the scaffold is also able to take the form and fill the excised NP cavity. Additionally, pre-formed scaffolds must be porous enough to allow cells to infiltrate and typically contain larger pore sizes, which do not effectively contain cells and ECM molecules and have been observed to lose the majority of synthesized molecules when submerged in media [47]. Injectable scaffolds do not require large pore sizes as the cells are mixed in before the scaffold cures and the act of seeding the cells in this matter results in a more even distribution of cells. The porosity

of injectable gels can also be tailored to encourage native cell interactions and metabolic activity and retain newly formed PGs [48].

Though injectable scaffolds for NP application offer advantageous characteristics, setting temperature and time as well as solution viscosity must also be considered in order to develop a solution that cures in a reasonable amount of time and at physiologically appropriate temperatures. Feasibility during injection and the ability to effectively remain in the NP cavity without extrusion before curing must also been considered [49, 50].

2.7 Hyaluronan and Elastin in the Intervertebral Disc

2.7.1 Hyaluronan

Hyaluronan (HA) is a glycosaminoglycan (GAG) found in the ECM with well-established biological roles. It is a linear copolymer formed from repeating disaccharide units of D-glucuronic acid and N-acetyl-D-glucosamine. As a polydisperse molecule, HA is distinctive from other GAGs with ranging molecular weights between 1 000 to 100 000 kDa [51]. HA is also the only GAG that is non-sulphated and is not attached to a protein core to form proteoglycans. As well, HA is formed at the inner face of the plasma membrane with the addition of sugars at the reducing end [52].

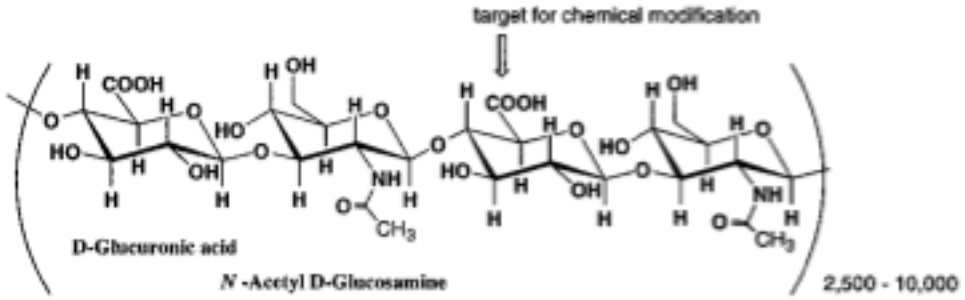

Figure 2-6. Structure of native hyaluronan [53].
Image used with permission: American Chemical Society, copyright 1997.

Located in nearly every mammalian tissue and fluid [44], HA is particularly abundant in synovial fluid of joints, vitreous fluid of the eye and in all cartilage types. Due to the variability in HA size, it can simultaneously interact with many cells through receptors or from forming complexes with other ECM molecules. Interactions with ECM proteoglycans, aggrecan and link proteins allow HA to influence signal transduction, cell migration and cell proliferation [54]. Many functions of HA involve interactions with CD44, a cell-surface receptor. CD44 is a cellular hyaladherin protein that binds to HA through the link module, a common amino acid globular binding domain [51]. HA interactions are important for the mechanical load-bearing role in cartilage and NP tissue.

2.7.2 Hyaluronan in the Intervertebral Disc

In the IVD, HA interacts with aggrecan to retain PGs and stabilizing the ECM. Through the binding of aggrecan monomers, HA can form large non-dissociable aggregates that contribute to the IVD structure by imparting the ability to resist compression [55].

HA is naturally degraded by hyaluronidases (HAses). As degradation occurs HA in the ECM is replaced by HA of a smaller mass resulting in a decrease in molecular

weight with age, though with an overall increase of HA concentration [55]. The aggregate components in HA that have formed a large aggregate complex are able to withstand endocytosis, but are catabolized within the ECM. HA not attached to a large aggregate or if attached to small degraded aggregate fragments, is endocytosed by the cells and degraded within the lysosome. With the onset and progression of DDD, the aggrecan that binds to HA decreases in both size and amount and the endocytotic process and subsequent degradation enhance the effects of degeneration [55].

2.7.3 Modified Hyaluronan

There are many issues surrounding the use of HA as a material for tissue engineering, some of which involve extrusion of material, toxic crosslinking agents or by-products and poor biomechanical properties [56].

The Prestwich group at the University of Utah has produced a thiol-modified HA (TMHA) that may offer a solution to these issues. The THMA is a proprietary thiol-modified carboxymethylated HA that has been modified to allow for additional carboxyl groups. These additional carboxyl groups provide extra sites for thiol-modification and enhance the concentration and rate of disulfide bond formation, speeding up and allowing for more robust crosslinking [57]. The TMHA has a backbone M_w of approximately 200kDa and M_n of approximately 100kDa [58]. The additional crosslinking sites were created by attaching an additional carboxylic acid group to each glucosamine unit [58]. Briefly, HA has repeating units of D-glucuronic acid and N-acetyl-D-glucosamine with one carboxylic acid group in D-glucuronic acid, however, with the addition of a

carboxylic acid group to each glucosamine unit, the number of sites available for crosslinking can be increased. By adjusting the pH, the hydroxyl group in the glucosamine can be deprotonated and then reacted with chloroacetic acid to form the additional carboxylic acid group [58]. The carboxylic acid group is then thiolated by a reaction with 3-thiopropanoyl hydrozide [58]. The degree of thiolation can be measured using a modified Ellman method and for the TMHA used in this work, the number of thiols per 100 disaccharide units was 42% [58]. The TMHA can be crosslinked without toxic agents and with no toxic degradation by-products [59, 60]. In the presence of air, TMHA will form crosslinks because of the disulfide linkage, however, the rate of TMHA crosslink reaction is quite slow (4-6 hours) [61]. PEGDA, formed from a polyethylene glycol (PEG) backbone (molecular weight approximately 3500Da) has an acrylate group attached at each chain end [58], and is able to rapidly crosslink TMHA (within 10 minutes) via a Michael-type addition reaction between free thiols of the TMHA and acrylate groups of PEGDA [61]. This crosslinked hyaluronan has also been shown to increase residence time within scaffolds and to contribute to increased mechanical strength. It can be produced in injectable solutions that are able to cure *in situ* and form hydrogels [56]. TMHA has also demonstrated biocompatibility with regard to cell viability and function without causing adverse effects [56]. Tissue engineering studies using TMHA demonstrate reduced healing time in tympanic membrane healing and a reduction of post-operative intra-abdominal adhesion formation [62, 63].

2.7.4 Hyaluronan in Nucleus Pulposus Tissue Engineering

HA is an attractive candidate for NP tissue engineering as it is naturally produced in the body and influences many cellular interactions, including morphogenesis, inflammation and wound repair [64]. HA hydrogel solutions have the ability to be fluid enough to be injected into an NP cavity yet can be manipulated to become viscous and cure *in situ.* HA contributes to the creation of a biologically relevant matrix, sharing attributes of a normal IVD ECM and has also been observed to interact with CD44 receptors and stimulate proliferation and PG production [65]. Studies involving unmodified HA have shown promise with regards to cell viability [66], however, low HA retention due to rapid degradation and high solubility has been shown to lead to a loss of cells through injection site, limiting the potential of an HA gel as a cell carrier [67].

A more promising option involves incorporating HA into a scaffold. In a study by Stern and others, porcine disc cells were seeded into a fibrin/HA scaffold and gelled with the addition of thrombin [65]. PG synthesis measured in the alginate gel scaffold (control) and fibrin/HA scaffold demonstrated higher PG synthesis along with retention of the disc cell phenotype in the fibrin/HA scaffold [65]. In a study by Halloran and others, bovine nucleus pulposus cells were seeded into scaffolds formed from atelocollagen type II, aggrecan and HA crosslinked with mTGase [68]. This crosslinked scaffold demonstrated the ability to support NP cells and express normal cell phenotype and also had the lowest elution of sulfated GAG into the surrounding environment when compared to non-cross-linked scaffolds [68].

2.7.5 Elastin

Elastin, or the elastin fibre, is an important ECM molecule and confers the property of elastic recoil, resuming shape after stretching or contracting. The structure of elastin fibres provides stable structural support and extensibility.

The elastin fibre (elastin) is composed of crosslinked elastin protein and the multicomponent microfibrils. The elastin protein itself is formed from tropoelastin monomers and subsequently crosslinked by lysyl oxidase [69]. Tropoelastin is characterized by alternating regions of hydrophobic amino acids and lysine rich regions [70]. Covalent crosslinkages stabilize the polymer and are formed through side chain lysine residues following oxidative deamination via lysyl oxidase [71]. Elastin degradation is slow, but occurs naturally through proteolytic degradation via elastase.

Elastin is produced naturally in the body and has beneficial regulatory functions in the vascular system [72]. Typically acting with collagen, elastin confers structural integrity in regions where elasticity is needed such as in the lungs, major blood vessels and the skin. The elastic property of elastin, and its biocompatibility offers useful characteristics for biomedical applications. The elastin protein and elastin-like polypeptides have been studied for applications in vascular grafts, drug delivery and cartilage repair [73, 74, 75, 76].

2.7.6 Elastic Fibres in the Intervertebral Disc

It was previously believed that elastic fibres did not play any significant role in the mechanical function of the IVD due to their sparse and sporadic distribution within the IVD [77]. However, recent studies of elastic fibres in the IVD offer interesting revelations, which indicate that elastic fibres may be an important component of the disc. In a study by Yu and others, an organized network of elastic fibres was observed in adolescent human IVD and was noted to be sparse and disrupted in scoliotic discs, suggesting that the elastic fibre network plays a biomechanical role in the IVD [78]. This is consistent with results from Smith and Fazzalari where greater concentrations of elastic fibres were observed in areas of the disc subject to the greatest tensile deformation [79].

Elastic fibres are distributed radially in the nucleus and at the NP/AF interface suggesting a role in maintenance of the NP structure and contributing to the resistance of tensile forces and also to the recovery after deformation [80]. Findings by Cloyd and others also demonstrate a link between elastin and aging and degeneration, where no differences in elastin content was distinguishable between inner and outer AF or NP in non-degenerate discs, but in degenerated discs the inner AF had significantly greater elastin content, correlating elastin content to degeneration and age [77]. The findings from these studies have altered the consideration of elastin as a factor contributing to mechanical function in the IVD where further studies will provide greater insight into the biological role of elastin in the disc.

2.7.7 Elastin-like Polypeptides

While elastin confers characteristics such as elasticity and resiliency that may be advantageous for biomedical applications, current inefficient methods for native elastin extraction limit this possibility. An alternative to the use of native elastin is the production of synthetic elastin-like polypeptides (ELP). Bellingham and others have been able to fabricate a polymeric matrix with solubility and mechanical properties similar to native elastin through the use of recombinant polypeptides based on human elastin sequences [81]. The recombinant ELP are similar in form to tropoelastin in that they are composed of hydrophobic domains rich in non-polar amino acids alternating with crosslinking domains rich in alanine and lysine residues [82]. The ELP to be utilized in this work is EP4 or EP 20-24^4 which is in reference to the sequence of exons: 20-21-23-24-21-23-24-21-23-24-21-23-24. Naming notion refers to the hydrophobic domains in the polypeptide, where exons 20 and 24 are hydrophobic domains and exon 24 is most frequently repeated, as is the case in human elastin [83]. Exons 20 and 24 are typically rich with glycine, valine and occasionally alanine [83]. The crosslinking domains are exons 21 and 23 most often rich with alanine and lysine [83]. Accordingly, all four of the exons, 20, 21, 23 and 24 can be found in native human elastin [83].

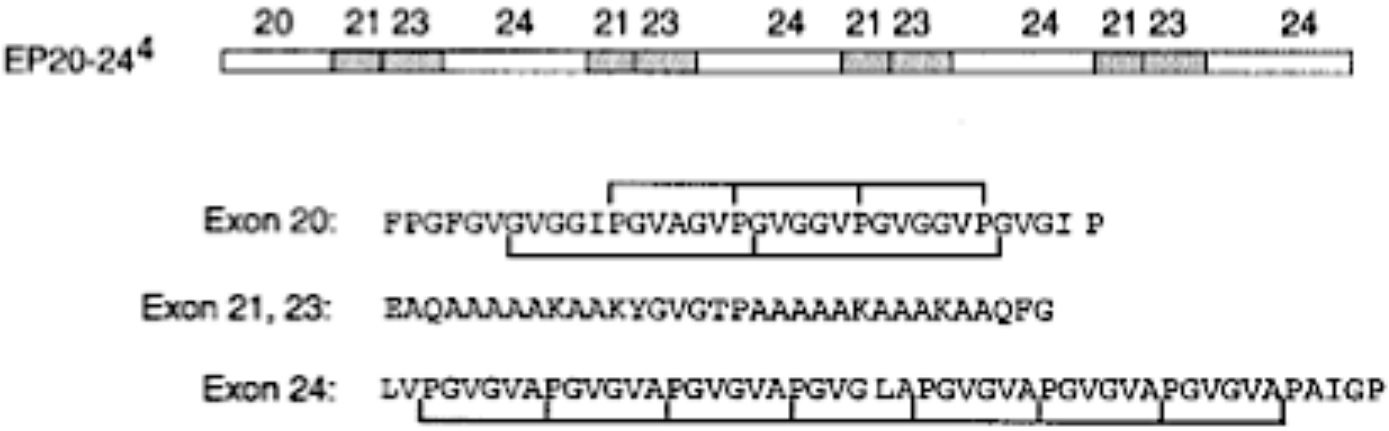

Figure 2-7. Elastin-like polypeptide structure and amino acid composition. Crosslinking exons are shaded. Brackets indicate repeating peptide motifs [81]. Imaged used with permission from: Wiley-Periodicals, copyright 2003.

Tropoelastin and elastin-like polypeptides have the ability to self-aggregate through coacervation *in vitro* [81]. Coacervation is a reversible temperature induced phase separation (TIPS) process important for elastin fibrillogenesis. Upon an increase in temperature, the protein in solution form molecular aggregates, separating from the solvent as a second phase [84]. At temperatures below the coacervation temperature, ELPs are soluble in aqueous solutions and at temperature above ELPs coacervate and organize into fibres. Materials composed of crosslinked ELP demonstrate remarkable similarity to native insoluble elastin in elastic modulus, extensibility to failure and energy loss in loading-unloading (resilience) cycles [81].

2.7.8 Elastin-like Polypeptides in Tissue Engineering

Though studies of ELP for NP tissue engineering have been limited, ELPs have demonstrated potential as non-thrombogenic coatings in vascular grafts and as a vehicle

for drug delivery [73, 75]. The ELP is biocompatible and coacervation can be manipulated to be used advantageously for tissue engineering applications [85, 86]. Biomedical studies utilizing ELPs suggest ELPs promote a chondrocytic-like phenotype in cartilaginous tissue repair and have the ability to stimulate chondrocytic differentiation of human adipose derived stem cells, demonstrating the potential of ELPs in tissue engineering applications [87, 88].

2.7.9 Nucleus Pulposus Tissue Engineering using Modified Hyaluronan and Elastin-like Polypeptides

Separately, HA and ELP has shown potential as scaffold materials for tissue engineering [65, 68, 73, 75]. TMHA can be crosslinked with polyethylene glycol diacrylate (PEGDA) curing into a hydrogel with an ability to attract and retain water, producing a suitable 3D environment for NP cells [58]. Through only trace amounts of elastin are naturally present in the NP, elastin confers advantageous properties such as resiliency and elastic recoil that is beneficial to the normal load-bearing structure of the IVD [80]. Synthesized ELPs have demonstrated an ability to mimic the solubility and mechanical properties of native elastin [81]. For NP tissue engineering, each material by itself however, is not sufficient to mechanically support the normal loads placed upon the IVD. A scaffold that combines HA and ELP may offer a construct that is biologically relevant and may reinforce structural properties to mimic an environment similar to native disc. HA and elastin are both found within the disc ECM and are both essential to normal disc functions [64, 65, 72]. Both materials have demonstrated potential in the maintenance of chondrocytic-like phenotypes, suggesting promise in the production of normal disc ECM molecules [65, 68, 87, 88]. In addition, TMHA and EP4, the specific

ELP to be utilized in this research, exist in solution at room temperature enabling homogenous cell seeding and distribution and curing of the hydrogel occurs after *in vitro* or *in situ* at physiological temperatures.

Chapter 3 Material and Methods

3.1 ELP Synthesis and Purification

Elastin Specialties Inc. (Toronto, Ontario) provided the elastin-like polypeptide utilized in this research. Using recombinant DNA technology. Briefly, ELP was synthesized through fermentation using *E.Coli* for protein expression and induction following the methods of Bellingham and others [82]. An ion-exchange column was used to separate the ELP from the bacterial host proteins. Purified ELP were fractions were pooled and dialyzed in acetic acid before storage at -20C or lyophilized.

3.2 Cyclic Hydrostatic Loading

The custom made hydrostatic pressure system (Tissue Growth Technologies, Minnetonka, Minnesota) was designed to apply cyclic hydrostatic loading to the NP seeded scaffold to mimic the mechanical stresses placed on the IVD in order to evaluate the efficacy of the TMHA and 3:1 TMHA/ELP scaffolds for NP tissue engineering. The system was set up by attaching a 25N load cell to the actuator of the servoelectric micromechanical testing device (TestResources Inc, Shakopee, Minnesota) to which the pressure generation cylinder was connected. The pressure generation cylinder sat atop the steel standoff base, which was secured to base of the microtester frame and secured in place with 2 C-clamps. The pressure tubing from the pressure generation cylinder connected the pressure generation cylinder to the hydrostatic pressure chamber housing the samples, with a pressure sensor connection branching off from the tubing and

interfaced with the computer. The hydrostatic pressure chamber was held in place with a retort stand and submerged in a water bath filled with 37°C water. Using the microtester software, a program was coded that subjected the samples to cyclic loading at 1MPa (~145psi) at 1 Hz for 3 hours a day. Cyclic loading was applied for 3 hours a day for 3 consecutive days and media was changed every day.

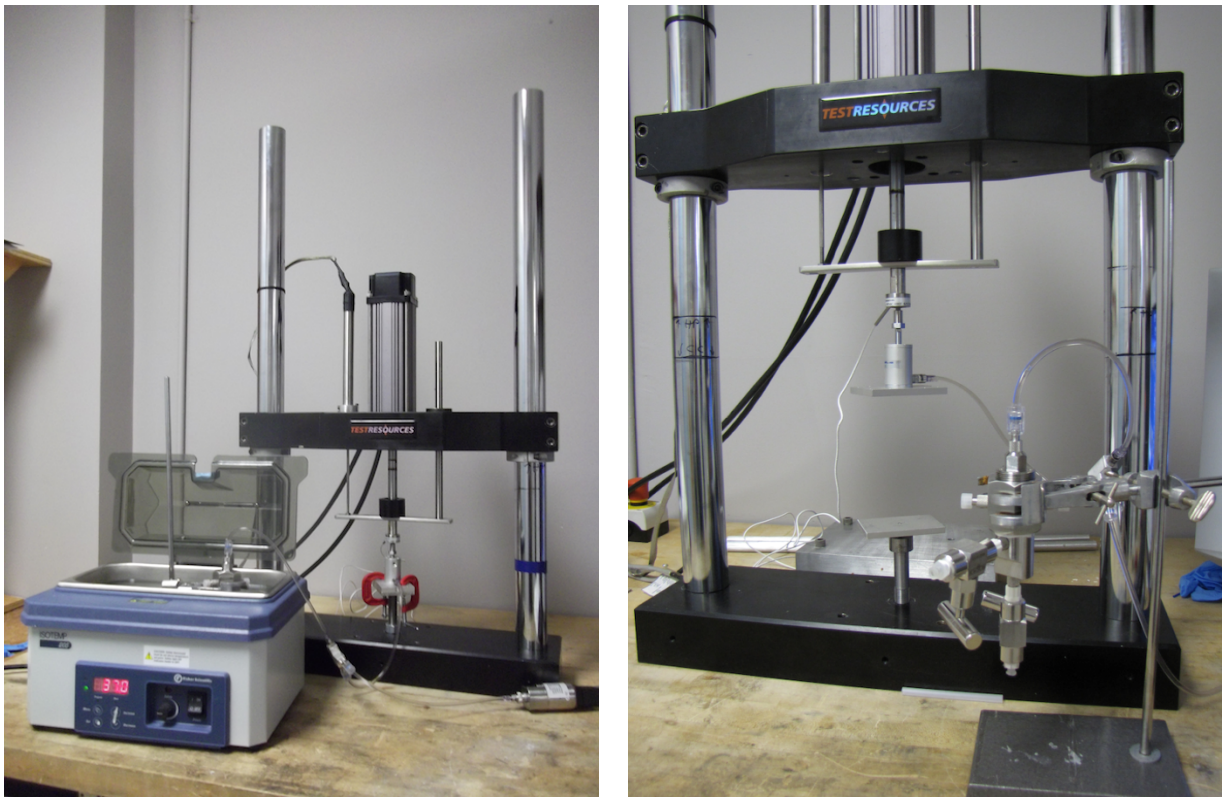

Figure 3-1. Hydrostatic pressure system set-up (left) and close-up of hydrostatic pressure chamber (right).

3.3 Cell Source

IVD specimens from patients undergoing spinal surgeries were obtained from Dr. Albert Yee (Sunnybrook Health Sciences Centre, Toronto) following appropriate institutional review board approval. Disc samples were obtained from male and female

patients between the ages of 29-82 typically following nucleotomy. Samples were covered with Dulbecco's Modified Eagle's Medium (DMEM; Wisent, Inc., St. Bruno, Quebec, Canada) with 1% penicillin/streptomycin (P/S; Wisent Inc., St. Bruno, Quebec, Canada) and 10% fetal bovine serum (FBS; Wisent, Inc., St. Bruno, Quebec, Canada) and incubated overnight at 37°C and 5% CO_2.

3.4 Disc Digestion and Culture

Following the protocol of Chiba and others [89], the IVD cells were isolated. The specimen was washed twice with PBS and morselized into fine fragments using a scalpel and forceps. The specimen was then subject to the first phase of enzymatic digestion with pronase digestion medium. Pronase digestion medium was concocted as 4mg/mL pronase (Calbiochem, San Diego, California), 0.04mg/mL DNase I, Grade II (Roche Applied Science, Basel, Switzerland) in DMEM with 1% P/S and 10% FBS and sterile-filtered. (If sample mass was greater than 1.5g, the sample was split into two with 10mL each of digestion medium, otherwise, sample was suspended in 20 mL digestion medium). The sample was placed in an incubated shaker at 37°C at 180 rpm for 90 minutes. Following pronase digestion, the sample was centrifuged at 1000 rpm for 10 minutes after which the supernatant was aspirated. Centrifugation was repeated twice, washing with PBS each time. The sample was then subject to the second phase of enzymatic digestion with collagenase digestion medium. Collagenase digestion medium was prepared with 0.12mg/mL of collagenase type II (Sigma Aldrich, St. Louis, Missouri) and 0.04 DNase I, Grade II in DMEM with 1% P/S and 10% FBS. The sample was placed in an incubated shaker at 37°C at 180 rpm for 3 hours. Following collagenase

digestion, the sample was centrifuged as per above, but after the final spin, was resuspended in 19mL DMEM with 1% P/S and 10% FBS and 1mL of 75ug/mL ascorbic acid (Sigma Aldrich, St. Louis, Missouri). The sample was passed through a 70μm cell strainer and cells were counted with a hemacytometer and plated in a vented tissue culture polystyrene flask for monolayer expansion. Cells were cultured at 37°C and 5% CO_2, passaging at approximately 85-90% confluency (not exceeding 4 passages) and medium was changed every other day.

3.5 Cell Source

IVD specimens from patients undergoing spinal surgeries were obtained from Dr. Albert Yee (Sunnybrook Health Sciences Centre, Toronto) following appropriate institutional review board approval. Disc samples were obtained from male and female patients between the ages of 29-82 typically following nucleotomy. Samples were covered with Dulbecco's Modified Eagle's Medium (DMEM; Wisent, Inc., St. Bruno, Quebec, Canada) with 1% penicillin/streptomycin (P/S; Wisent Inc., St. Bruno, Quebec, Canada) and 10% fetal bovine serum (FBS; Wisent, Inc., St. Bruno, Quebec, Canada) and incubated overnight at 37°C and 5% CO_2.

3.6 Disc Digestion and Culture

Following the protocol of Chiba and others [89], the IVD cells were isolated. The specimen was washed twice with PBS and morselized into fine fragments using a scalpel and forceps. The specimen was then subject to the first phase of enzymatic digestion with pronase digestion medium. Pronase digestion medium was concocted as 4mg/mL

pronase (Calbiochem, San Diego, California), 0.04mg/mL DNase I, Grade II (Roche Applied Science, Basel, Switzerland) in DMEM with 1% P/S and 10% FBS and sterile-filtered. (If sample mass was greater than 1.5g, the sample was split into two with 10mL each of digestion medium, otherwise, sample was suspended in 20 mL digestion medium). The sample was placed in an incubated shaker at 37°C at 180 rpm for 90 minutes. Following pronase digestion, the sample was centrifuged at 1000 rpm for 10 minutes after which the supernatant was aspirated. Centrifugation was repeated twice, washing with PBS each time. The sample was then subject to the second phase of enzymatic digestion with collagenase digestion medium. Collagenase digestion medium was prepared with 0.12mg/mL of collagenase type II (Sigma Aldrich, St. Louis, Missouri) and 0.04 DNase I, Grade II in DMEM with 1% P/S and 10% FBS. The sample was placed in an incubated shaker at 37°C at 180 rpm for 3 hours. Following collagenase digestion, the sample was centrifuged as per above, but after the final spin, was resuspended in 19mL DMEM with 1% P/S and 10% FBS and 1mL of 75ug/mL ascorbic acid (Sigma Aldrich, St. Louis, Missouri). The sample was passed through a 70μm cell strainer and cells were counted with a hemacytometer and plated in a vented tissue culture polystyrene flask for monolayer expansion. Cells were cultured at 37°C and 5% CO_2, passaging at approximately 85-90% confluency (not exceeding 4 passages) and medium was changed every other day.

3.7 Cell Characterization- Flow Cytometry

At approximately 90% confluency, cells were prepared for flow cytometry analysis to assess cell population and purity. Cells were washed twice with PBS and

trypsinized with 3mL of 0.05% trypsin with EDTA. After incubation at 37°C, 5% CO_2 for 4 minutes, trypsinization was neutralized with 5mL of DMEM (1% P/S, 10% FBS) and centrifuged for 5 minutes at 600 rpm. Supernatant was removed and cells were resuspensed in a solution of 0.1% BSA solution. Cells were counted with a hemacytometer and 2 filtered falcon tubes were filled with approximately 10^6 cells/mL each. A volume of 7.5mL of CD24-antibody (BD Biosciences, Franklin Lakes, New Jersey) was added to one falcon tube with the second acting as the control. Samples were covered in aluminum and incubated for 30 minutes before running cytometric analysis using a BD FACSCalibur. Following flow cytometry analysis, nucleus pulposus cell samples were stained using the Giemsa-Wright stain to further visualize NP cell morphology. Cell samples were allowed to air dry on a microscopy slide and dipped in the Giemsa-Wright (Invitrogen, Carlsbad, California) stain for 3 minutes. Excess dye was carefully blotted away and the slide was dipped in a buffer solution before excess residual dye and buffer solution was rinsed away. The slide was set aside to air dry before being visualized under 20x objective on the Carl Zeiss inverted Axiovert microscope (Carl Zeiss, Germany).

3.8 Gel Preparation and Cell Encapsulation

The 3:1 TMHA/ELP ratio was selected based on encouraging results for cell viability and phenotypic expression from previous research [90]. The TMHA hydrogel served as a control. Cells were washed twice with PBS before being trypsinzed for 4 minutes with 3mL of 0.05% trypsin in EDTA at 37°C, 5% CO_2. The trypsin was then neutralized with 7mL of DMEM with 1%P/S, 10% FBS and centrifuged at 600 rpm for 5 minutes. Cells

were counted with a hemacytometer and resuspended at approximately 10^6 cells/mL in DMEM with 1% P/S, 10% FBS. Following the protocol of Moss [90], the gels were encapsulated. TMHA (Glycosan BioSystems Inc., Salt Lake City, Utah), ELP (Elastin Specialties Inc., Toronto, Ontario) and PEGDA (Laysan Bio inc., Arab, Alabama), were all dissolved in serum-free DMEM with 1%P/S to achieve a final solution of 15mg/mL, 40mg/mL and 40mg/mL respectively. The TMHA was placed in the incubator at 37°C, 5% CO_2 for 45 minutes. The pH of the ELP solution was adjusted to approximately 7 with 2M NaOH and then sterile-filtered. TMHA and 3:1 TMHA/ELP scaffolds were formed by combining the TMHA, ELP, PEGDA and cell suspensions according to Table 3-1 into 8-well borosilicate chamber.

Hydrogel Components	Hydrogels			
	TMHA	TMHA control	3:1	3:1 control
TMHA (vol, conc)	270µL, 1.8%	270µL, 1.8%	230µL, 2.1%	230µL, 2.1%
ELP (4% w/v)	----------	----------	40µL	40µL
NP cells (10^6 cells/50µL)	50µL	----------	50µL	----------
DMEM (1% P/S)	----------	50µL	----------	50µL
PEGDA (4% w/v)	80µL	80µL	80µL	80µL

Table 3-1.TMHA and 3:1 TMHA hydrogel formulations

The scaffolds were allowed to gel for 2 hours at 37°C, 5% CO_2 and then transferred into mesh inserts, placed into the main chamber of the hydrostatic pressure chamber and covered with 3mL of DMEM (1%P/S, 10%FBS) and 75ug/mL ascorbic acid. Scaffolds were cultured for 4 days, changing the media every day and subject to hydrostatic pressure cycling at 1MPa for 3 hours a day for 3 days. The experiment was

repeated three times with hydrostatic pressure loading and without loading to act as a control.

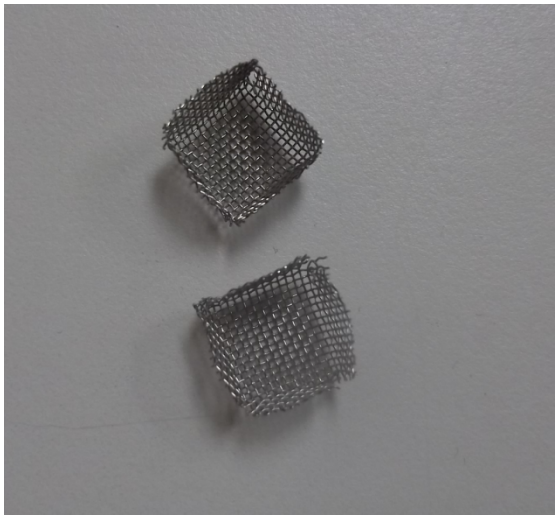

Figure 3-2. NP-seeded hydrogels are placed in mesh inserts before stacked one-atop-another inside the main chamber hydrostatic pressure chamber.

Figure 3-3. Mid-chamber (left) and main chamber (right) that comprise the hydrostatic pressure chamber.

3.9 Cell Viability

At day 1 (day of cell encapsulation) and at day 4, both ratios for loaded and unloaded trials, were subject to cell viability assessment. Scaffolds were placed in a Lab-Tek chambered borosilicate coverglass slide and covered with 200µL of DMEM (1%P/S, 10%FBS), 150µL of 10µm solution of Calcein AM and 100uL of 1µm solution of Sytox. The scaffolds were covered with aluminum for 30 minutes before imaging.

Images were visualized under a 10x objective on the Carl Zeiss inverted Axiovert microscope (Carl Zeiss, Germany). Live cells fluoresced green and dead cells fluoresced red when viewed using the FITC and Rhodamine filters. In total, 40 Z-stack images were captured for each sample, spaced 5µm apart to visualize a total 200µm of each gel. The number of green and red cells was counted in every 5 slices using Axiovision LE (Axiovision software for viewing images). The number of live and dead cells was expressed as a percentage of the total.

After imaging, samples were homogenized in 1mL of TRIzol Reagent in a Potter-Elvehjem Tissue Grinder and frozen at -80°C until gene expression analysis.

3.10 Gene Expression

At day 1 and 4 for both loaded and unloaded TMHA and 3:1 TMHA/ELP scaffolds, gene expression was evaluated. In particular, 5 different genes relevant to the NP cells were analyzed: SOX9, CD24, collagen type I, collagen type II and aggrecan. GAPDH and 18S, two housekeeping genes, were also included.

Gene expression analysis was conducted in a designated PCR area using certified RNase-free pipet tips and microtubes. RNA extraction was performed following the TRIzol Reagent protocol and the Qiagen RNeasy kit protocol. Samples were thawed at room temperature to permit complete dissociation of nucleoprotein complexes. A volume of 200µL of chloroform was added to each sample. The tube housing each sample was shaken vigorously for 15 seconds and let to sit for 2-3 minutes at room temperature. Samples were centrifuged at 12 000 x g for 10 minutes at 4°C to separate the RNA (upper aqueous phase) from the phenol-chloroform. RNA was precipitated out by transferring upper aqueous phase into a fresh tube and adding 500µL of isopropyl alcohol. Samples were allowed to sit for 10 minutes at room temperature and then centrifuged at 12 000 x g for 10 minutes at 4°C. After centrifugation, the supernatant was removed and the RNA pellet washed thoroughly by pipeting up and down with 1mL of 75% ethanol (prepared with RNase-free water). In an RNeasy spin column, 500µL of the sample was transferred over and centrifuged at 8 000 x g for 15 seconds at 4°C after which, the flow-through was discarded. This step was repeated with the remaining 500µL sample. The sample was then washed with 500µL of Buffer RPE, centrifuged for 15 seconds at 8 000 x g at 4°C and then transferred into a new collection tube before being centrifuged for another 30 seconds at the same settings. The RNA was eluted by adding 30µL of RNase-free water and centrifuging for another minute at 8 000 x g at 4°C.

Reverse transcription was carried out according the Qiagen Omniscript RT kit protocol. The 10x Buffer RT, dNTP mix (5mM), oligo-dT, RNase inhibitor, Omniscript

RT and template RNA were all thawed and stored on ice. The RNase inhibitor was diluted to a final concentration of 10μL/μL in 1x Buffer RT (10x Buffer diluted with RNase-free water). Master mix was prepared accordingly per sample and samples were then incubated at 37°C for an hour.

MASTER MIX:

Component	**Volume/reaction**
10x Buffer RT	2μL
dNTP Mix	2μL
Oligo-dT	2μL
RNase-inhibitor	2μL
Omniscript Reverse Transcriptase	1μL
Template RNA	10μL
Total volume	**22μL**

Table 3-2. Composition of master mix for carrying out reverse transcriptase.

PCR was conducted following the Qiagen Taq DNA Polymerase Protocol. The 10x PCR Buffer, dNTP mix, primer solutions Taq and template DNA were thawed on ice. The master mix per sample was prepared accordingly:

MASTER MIX:

Component	**Volume/reaction**
10x PCR Buffer	2μL
dNTP mix (5mM each)	0.5μL
Primer mix	0.5μL
Taq Polymerase	0.15μL
RNase-free water	15.85μL
Template DNA	1μL
Total Volume	**20μL**

Table 3-3. Composition of master mix for carrying out PCR.

The forward and reverse primers for all the genes analyzed were purchased from ACGT Corporation based on the designs by Moss [90]. Samples were placed into a Techne 20-well thermal cycler (Bibby Scientific Limited, Staffordshire, UK) and set according to the settings below:

Initial denature	95°C for 5 minutes
3-step cycling:	**40 cycles of:**
i. Denaturation	95°C for 30 seconds
ii. Annealing	60°C for 30 seconds
iii. Extension	72°C for 1 minute
Final extension	72°C for 5 minutes
Hold	4°C

Table 3-4. Thermal cycler program settings for running PCR.

Following PCR, samples were visualized on ethidium bromide-stained 2% agarose gels and imaged using an Alpha Imager EC UV lightbox (AlphainnoTec, Germany).

3.11 Statistical Analysis

Statistical analysis was performed using the statistical software SPSS. A Kruskal-Wallis test was performed to compare percentage cell viability among treatment groups. Least significant difference for ranks (LSD-ranks) was used to determine where statistically significant differences occurred between the specific groups. Statistical significance was assessed at $p=0.05$.

Chapter 4 Results

4.1 Cell Culture

Intervertebral disc samples were obtained from a total of 15 different patients undergoing surgery for disc degeneration over the course of 14 months (Table 4-1). Of the 15, 4 were utilized for training purposes, 2 were assessed via flow cytometry to be too low in CD24 expression and abandoned and 9 were used for encapsulation and subject to cyclic hydrostatic loading (Table 4-1). Samples varied in mass, ranging from 0.5g to over 7g and cell density yielded from each sample after disc digestion was also widely variable (between $3.0x10^5$ cells/mL to $2.7x10^6$ cells/mL).

Disc Number	Patient age (year)	Patient gender	CD24 characterization (%)	Purpose
1	Middle-aged	Male	Not conducted	Training
2	51	Female	Not conducted	Training
3	40	Male	Not conducted	Training
4	Middle-aged	Female	Not conducted	Training
5	Middle-aged	Male	98.8 CD24+	TMHA 3:1 TMHA/ELP
6	61	Male	97.9 CD24+	TMHA 3:1 TMHA/ELP
7	31	Male	8.53 CD24+	Not used
8	29	Female	92.4 CD24+	TMHA 3:1 TMHA/ELP
9	64	Male	50.9CD24+	TMHA
10	57	Female	1.55 CD24+	Not used
11	Mid-40s	Male	12.6 CD24+	TMHA 3:1 TMHA/ELP
12	82	Female	93.5 CD24+	TMHA
13	38	Male	87.8 CD24+	TMHA 3:1 TMHA/ELP
14	Mid-20s	Male	63.5 CD24+	TMHA 3:1 TMHA/ELP
15	50	Male	97.1 CD24+	TMHA 3:1 TMHA/ELP Control

Table 4-1. Summary of digested discs and characteristics of patient samples.

In culture, NP cells assumed a long and thin fibrocyte-like phenotype though once encapsulated in a 3D hydrogel environment, NP cells resumed a spherical and chondrocyte-like form (Figure 4-1).

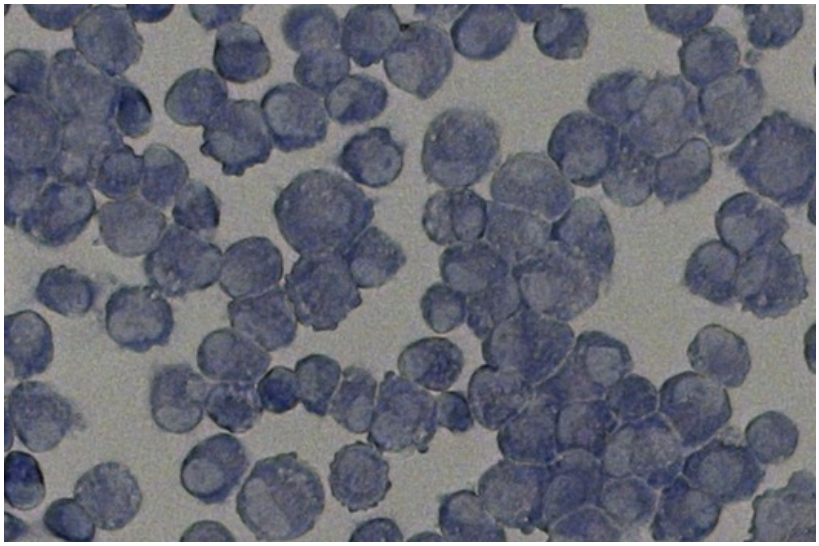

Figure 4-1. Wright-Giemsa stained nucleus pulposus (Objective: 20x on Axiovert Inverted Microscope).

4.2 Cyclic Hydrostatic Loading

There were significant issues experienced with the equipment and in particular challenges with pressure generation were observed. For these reason, out of 9 trials for cyclic hydrostatic loading, only 6 trials were usable due to inconsistent pressure output. Figure 4-2 displays variances in pressure generation during one day of cyclic hydrostatic pressure loading, specifically depicting erratic pressure generation with respect to displacement. The timeline of hydrostatic pressure set-up issues and unused cyclic loading experiments are included in Appendix A and B respectively. As a consequence of the challenges with the equipment, a report was prepared and sent to Tissue Growth Technologies to troubleshoot issues and is included in Appendix C. Briefly, there were

air bubble and leakage issues experienced with the equipment which likely lead to inconsistent and unpredictable pressure generation. Figure 4-3 shows cyclic hydrostatic pressure loading of one successful pressure experiment and this data is typical of the cyclic hydrostatic pressure loading that was applied to the remaining 5 successful trials.

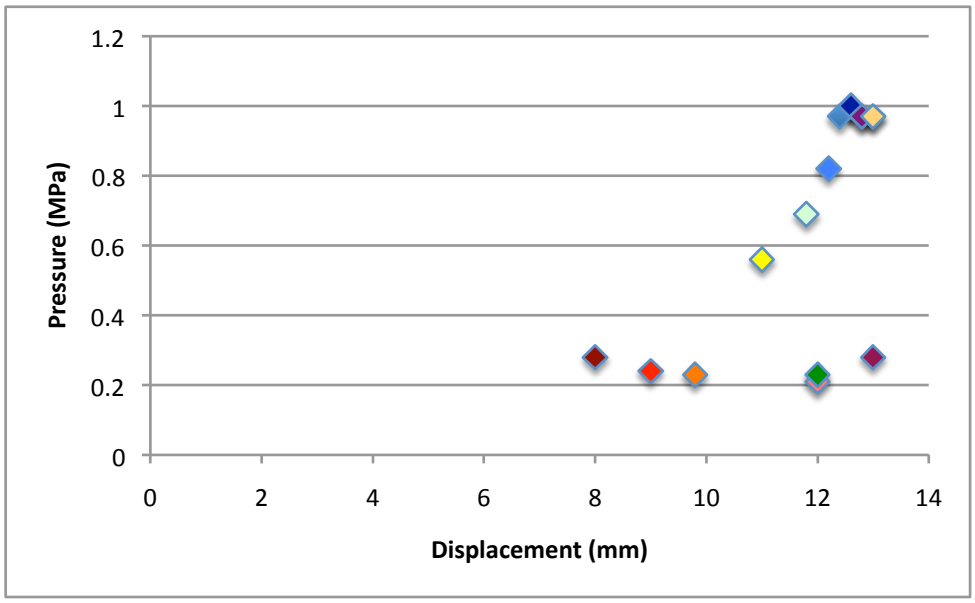

Figure 4-2. Variances observed in cyclic hydrostatic pressure generation with respect to displacement during one pressure generation session. Each coloured point represents individual 35-second pre-test cyclic pressure generation cycles within the 1-day trial session.

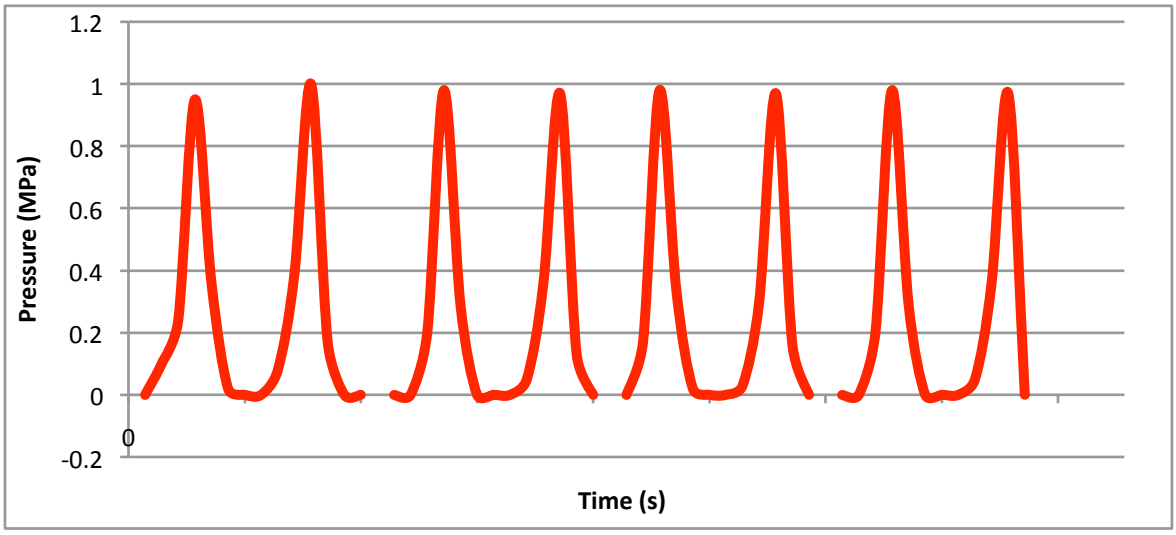

Figure 4-3. Cyclic hydrostatic pressure data from one 3-hour pressure generation session typical of the cyclic hydrostatic pressure data from the 6 successful pressure application experiments.

4.3 Cell Viability

Triplicate sets of each hydrogel ratio and treatment group were undertaken. Microscopy imaging of the NP cell-encapsulated hydrogels indicated relatively even distribution and chondrocyte-like spherical morphology representative of NP cells. Imaging showed a decreasing trend in cell viability from day 0 (Figure 4-4B and C) to day 4 (Figure 4-4D, E, F, G) regardless of hydrogel ratio or cyclic hydrostatic pressure treatment.

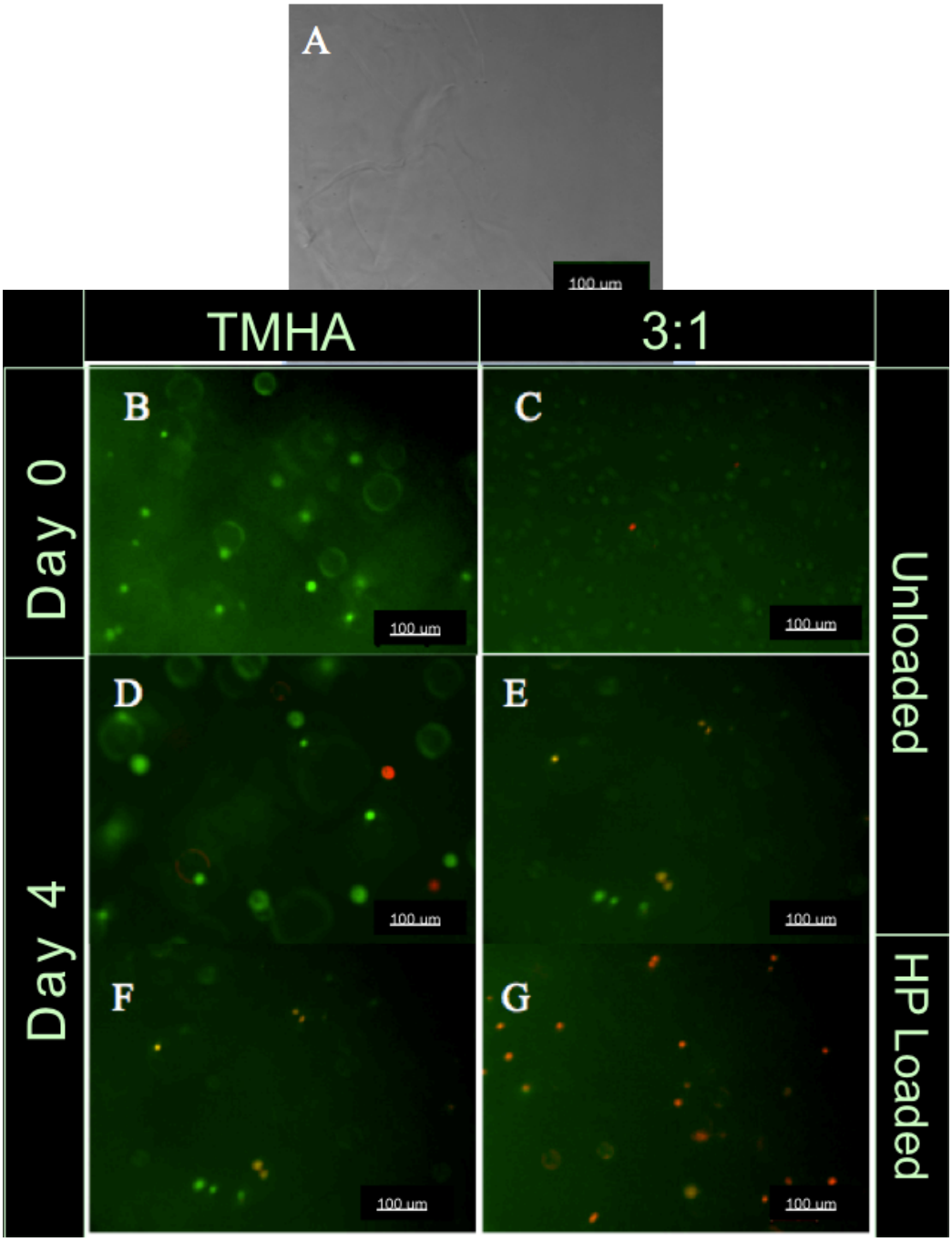

Figure 4-4. Live/Dead image of NP cells in TMHA/ELP hydrogels. Live cells fluoresce green, dead cells fluoresce red. A) Control hydrogel (no cells seeded). B) TMHA-Day 0 and C) 3:1 TMHA/ELP-Day 0 unloaded hydrogel. D) TMHA-Day 4 and E) 3:1 TMHA/ELP-Day 4 unloaded hydrogel. F) TMHA-Day 4 and G) 3:1 TMHA/ELP-Day 4 loaded hydrogel.

The percentage viability within and between TMHA and 3:1 hydrogels at Day 0 and Day 4 in unloaded and loaded groups are shown in Figure 4-5. The percent in cell viability was found to be relatively consistent within the Day 0 unloaded treatment groups regardless of hydrogel ratio. The Day 4 unloaded and Day 4 loaded treatment groups indicated a greater variability in percentage cell viability within each group and between the two ratios of hydrogels (Figure 4-5). Kruskal-Wallis analysis indicated a statistical difference ($p<0.05$) and post hoc comparisons revealed a statistically significant difference between the TMHA-Day 0 unloaded treatment group and TMHA-Day 4 loaded treatment as well as between the TMHA-Day 0 unloaded treatment group and 3:1 TMA/ELP-Day 4 loaded treatment group. Though not statistically significant, there also seemed to be a strong decreasing trend in cell viability between Day 0 unloaded groups and Day 4 unloaded groups and from Day 4 unloaded groups to Day 4 loaded groups regardless of hydrogel ratio (Figure 4-5).

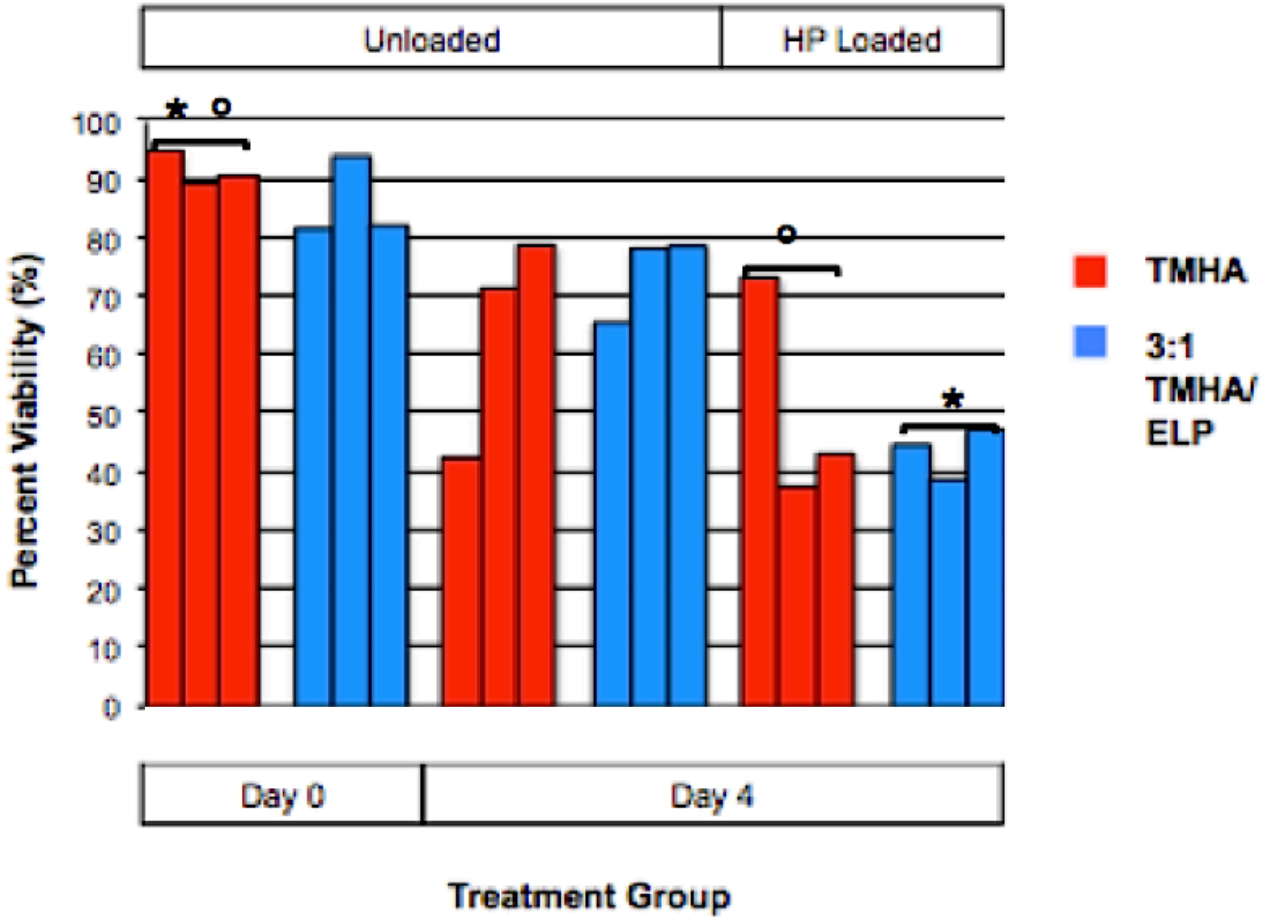

Figure 4-5. Percentage viability of NP-seeded cells in unloaded TMHA and 3:1 TMHA/ELP scaffolds at Day 0 and Day 4 and NP-seeded TMHA and 3:1 scaffolds at Day 4 after application of cyclic hydrostatic pressure. (T1, T2, T3 refers to triplicate trial repetitions for each treatment group). ° indicates statistically significant difference between the TMHA-Day 0 unloaded group and TMHA-Day 4 loaded group. * indicates statistically significant difference between the TMHA-Day 0 unloaded group and 3:1 TMHA/ELP-Day 4 loaded treatment group.

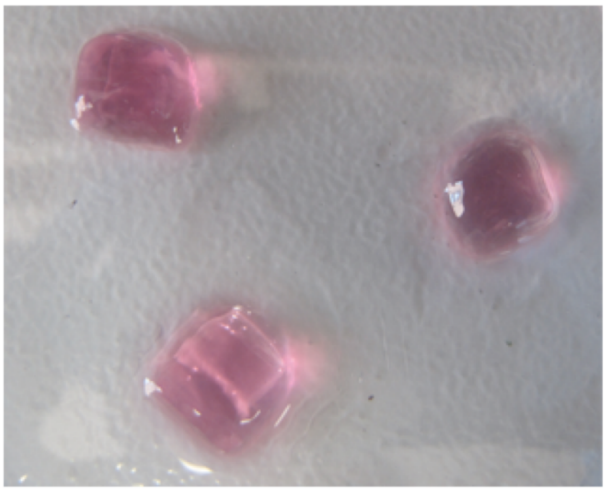

Figure 4-6. Nucleus pulposus cell encapsulated TMHA-based hydrogel scaffolds.

4.4 Gene Expression

RT-PCR results indicated variability among gene expression. Gene expression frequency is summarized in Table 4-2. Although all gels consistently expressed the 2 housekeeping genes, GAPDH and 18s (Figure 4-7A-G), and collagen type II gene expression was seen only in the control sample (Figure 4-7A). CD24 was apparent in the TMHA-Day 0 unloaded sample (Figure 4-7B) and only the 3:1-Day 0 unloaded treatment group (Figure 4-7E) showed a consistent frequency of SOX9 expression, which is an essential transcription factor for collagen type II synthesis and an important driver of the NP cell phenotype.

Gene	Monolayer (control)	TMHA			3:1 TMHA/ELP		
		DAY 0 unloaded	Day 4 unloaded	DAY 4 loaded	DAY 0 unloaded	DAY 4 unloaded	DAY 4 loaded
GAPDH	3/3	5/5	7/7	5/5	8/8	6/6	9/9
SOX9	0/3	0/5	0/7	0/5	7/8	0/6	0/9
CD24	0/3	2/5	0/7	0/5	0/8	0/6	0/9
Col I	0/3	0/5	0/7	0/5	0/8	0/6	0/9
Col II	2/3	0/5	0/7	0/5	0/8	0/6	0/9
Aggrecan	0/3	0/5	0/7	0/5	0/8	0/6	0/9
18s	3/3	5/5	7/7	5/5	8/8	6/6	9/9

Table 4-2. Summary of RT-PCR results indicating gene expression frequency from NP cells cultured in monolayer and TMHA and 3:1TMHA/ELP scaffolds.

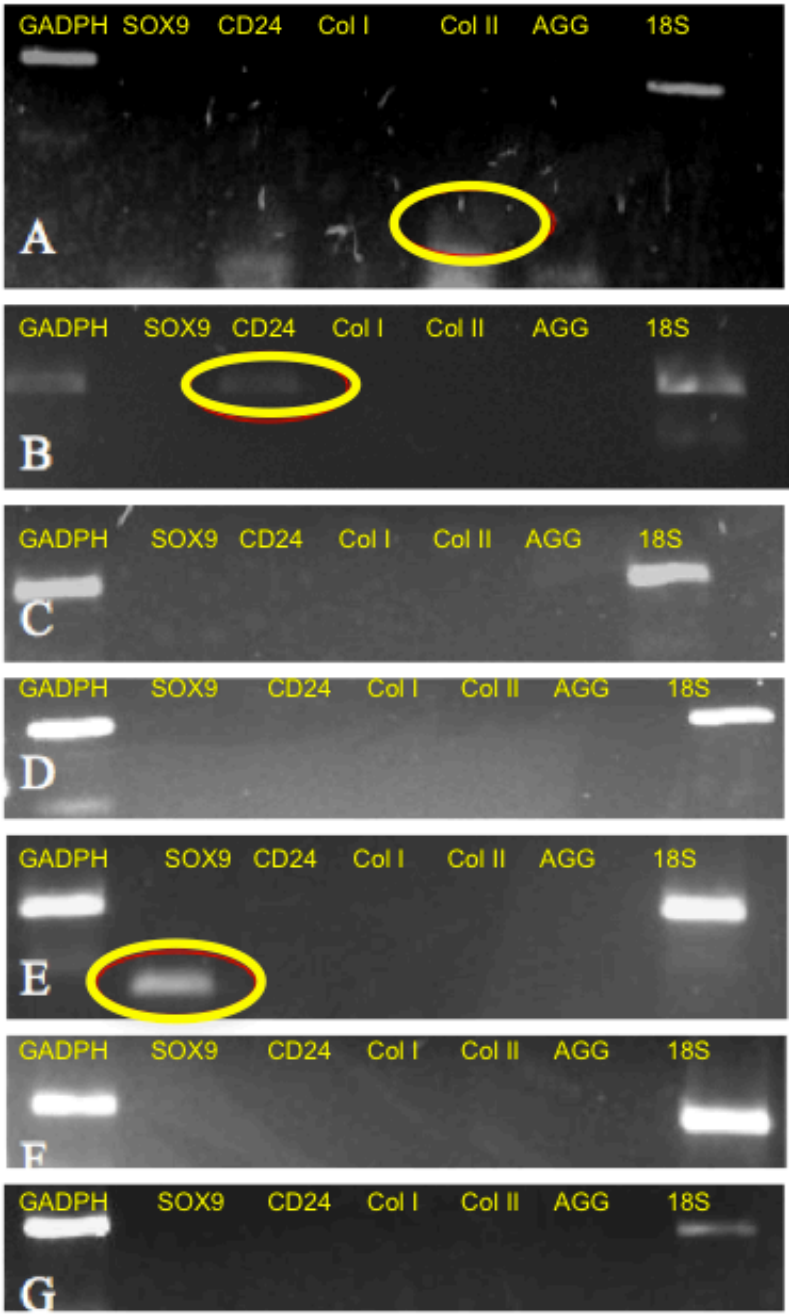

Figure 4-7. Agarose gels showing gene expression of Day 0 and Day 4 unloaded and loaded TMHA-based hydrogels. Two housekeeping genes, GAPDH and 18S are apparent in all samples (A-G). A) Collagen type II gene expression in the control sample. B) CD24 gene expression in the TMHA-Day 0 unloaded sample and E) SOX9 gene expression in the 3:1 TMHA/ELP-Day 0 unloaded treatment group.

Chapter 5 Discussion

5.1 Previous Work

Previous studies examining TMHA and ELP as a material for nucleus pulposus tissue engineering were inconclusive but indicated potential for a TMHA/ELP hydrogel formulation to support human nucleus pulposus cells [90,91]. Moss biomechanically assessed the TMHA/ELP formulations at 1:1, 2:1 and 3:1 via confined compression mechanical testing without cell encapsulation and although the 3:1 and 1:1 ratios revealed stiffness values stiffer than that of the TMHA hydrogel, the stiffness values for the 3:1 and the 1:1 were less than that reported in literature for native mammalian NP tissue [90]. However, the mean peak stress value of the 3:1 TMHA/ELP hydrogel fell within the range reported in literature for bovine nucleus pulposus and suggested a need for further investigation to assess the 3:1 TMHA/ELP hydrogel under cyclic loading conditions [90]. The experiments undertaken in this thesis were designed to determine the efficacy of a 3:1 TMHA/ELP ratio hydrogel with respect to NP cell support and viability following application of cyclic hydrostatic pressure. There are few studies that look at the effects of mechanical stimulation on NP-seeded hydrogel scaffolds for nucleus pulposus tissue engineering and to my knowledge, no previous studies have assessed the effects of cyclic hydrostatic loading on NP cells seeded in a TMHA and ELP composite hydrogel scaffold.

Moss prepared the TMHA in the TMHA and the 3:1 TMHA/ELP hydrogel formulations on a by-weight basis with a final concentration of TMHA at 1.5% w/v as

this was the mid-range of what had been used successfully by the Prestwich group. Higher TMHA concentrations tended to make the TMHA solution too viscous and difficult to handle [90]. Gelation time was manipulated by the addition of PEGDA, a thiol-reactive crosslinker, to cater to a suitable timeframe for *in situ* crosslinking applications. The PEGDA was combined in a 4:1 TMHA/PEGDA ratio. This ratio had the greatest efficiency in crosslinking TMHA [58]. This combination of TMHA and PEGDA demonstrated an ability to support human tracheal fibroblasts, where cells proliferated tenfold during a 4-week culture *in vitro* and secreted ECM *in vivo* in mice [58]. In keeping with the method by Moss, where findings revealed encouraging but inconclusive results, the preparation of 3:1 TMHA/ELP using a 4:1 TMHA/PEGDA ratio was used in this work.

5.2 Cell Source

Previous laboratory work demonstrated the ability of TMHA/ELP hydrogel formulations to support cultured NP cells [90. 91]. The results from the *in vitro* experiments in this research are consistent with previous work and showed similar ability in the TMHA and 3:1 TMHA/ELP hydrogels to support cultured NP cells. In culture, the NP cells displayed a long and spindle-like morphology and when encapsulated in the hydrogel, the cells exhibited a spherical morphology indicative of chondrocyte-like NP cells. This result suggested that neither the TMHA nor 3:1 TMHA/ELP hydrogel had a negative effect itself on cell viability, and live/dead staining and microscopy revealed a majority of the cells were alive. This finding is in agreement with the work of Moss where NP-cultured cells seeded in 3:1 TMHA/ELP hydrogels exhibited spherical

morphology at week 3 [90]. Windisch also observed similar results using a 1:1 TMHA/ELP hydrogel seeded with human NP cultured cells at day 14 [91]. Additionally, Sakai also noted rounded morphology and ECM production of human NP cultured cells after 14 days when seeded in an atelocollagen scaffolds [92].

The viability of the NP cells encapsulated in both hydrogel ratios decreased overtime which is not surprising as this study utilized excised disc material taken from patients undergoing surgery for disc degeneration. As the cells to be cultured and encapsulated were from a compromised environment, they may have decreased proliferative potential. This is consistent with work conducted by Moss and Windisch where cultured NP cells seeded in TMHA/ELP hydrogel formulations decreased in cell viability over the period of 3 weeks and 2 weeks respectively [90, 91]. As well, because all samples were taken from various patients differing in age and gender (Table 4-1), there is a great potential for variation in cell behaviour from donor to donor. Variability in cell behaviour also translated to a range of NP culture times. The issue with variable and possibly compromised cell sources may also have affected gene expression. In research by Kluba, NP cells cultured from degenerative tissues displayed a significantly lower level of collagen type II when compared with NP cells from healthy adolescent donors [93].

Disc samples used in this research were at times difficult to obtain due to patient recruitment and once digested, there was great variability in NP cells with regard to proliferation and culture time and susceptibility to infection. Windisch also experienced

issues with infection and variation in cell proliferation from human NP cells from disc samples obtained from degenerate sources [91]. Utilizing other cell types or a cell co-culture may provide greater potential to assess the efficacy of the TMHA and 3:1 TMHA/ELP hydrogels and to refine our understanding of the constituents of an effective regenerative therapy.

In research by Aguiar and others, increased proteoglycan synthesis was observed in bovine NP and canine notochordal co-cultured cells when compared to NP monoculture controls, suggesting the influence of notochordal cells on NP cells [94]. Erwin and Inman similarly noticed an influence of notochordal cells on NP cells, with an observed four-fold increase in cell proliferation in bovine NP and canine notochordal co-cultured cells compared to monoculture controls [95]. Whether this finding is translatable to human NP applications may require more investigation, as Le Visage and others demonstrated a significant increase in PG and GAG synthesis in human annulus fibrosus cells obtained from degenerate discs co-cultured with human mesenchymal stem cells, but no such increase was observed with co-cultured nucleus pulposus cells [96]. Mesenchymal stem cells may also be worth considering as Crevensten and others observed increased disc height and tissue resembling the native NP formation after injecting MSC-seeded hyaluronan scaffolds into rat discs models at 28 days [67].

5.3 Time Factors

In this research, NP cells were encapsulated for 4 days. Though during the span of 4 days, the cell viability decreased in both loaded and unloaded groups, it would be

interesting to see if the cells in either group would eventually recuperate if time had been extended beyond the 4 days or if this effect is observed in a TMHA/ELP scaffold with the incorporation of alternate cell type. In research by Crevensten, MSC-seeded HA gels were injected into rat coccygeal discs and 7-14 days after injection, injected stem cells were present but significantly decreased in amount [67]. After 28 days, there was a return to initial numbers of injected cells with 100% viability [67].

5.4 Scaffold Considerations

In previous research conducted, the 3:1 TMHA/ELP was determined as a starting point for assessing the efficacy of a TMHA and ELP composite scaffold for NP tissue engineering based on results from biomechanical evaluation in the absence of cells [90]. Results from previous research yielded positive results with regard to cell viability and morphology and with biocompatibility *in vitro* and *in vivo* respectively and biomechanically, the 3:1 TMHA/ELP ratio fell within the range for native NP peak stress reported in the literature [90]. However, the results from this research, where the cells were encapsulated into the scaffold and subsequently loaded, seem to indicate that the addition of ELP did not sufficiently impact the mechanical properties of the hydrogel scaffold to support viable NP cells.

As discussed above, cell source and variability in cell behaviour could have significantly impacted the findings and the mechanical properties of each the 3:1 TMHA/ELP hydrogel may be sufficient to support cell viability and phenotype if a different cell source were used. If it can be demonstrated that the 3:1 TMHA/ELP

scaffold is not sufficient to support healthy cells subject to cyclic hydrostatic pressure loading, other ratios may need to be investigated to determine the efficacy of a TMHA and EL4 composite scaffold for disc applications.

5.5 Hydrostatic Pressure Testing

The design of the hydrostatic pressure chamber was an issue that may also have impacted the results of this research.

The stainless steel chamber was made up of 2 components: the mid-chamber and the main chamber with the main chamber threaded into the mid-chamber. When the scaffolds were placed into the main chamber and threaded into the mid-chamber, it was very difficult to assess whether the scaffolds have been adequately covered with media. In pilot experiments, when the scaffolds were not sufficiently hydrated the hydrogels would shrivel up and provided a harsh environment for the cells.

The chamber also included two valve attachments so that media could be changed without taking apart the chamber. These valves were later omitted from the set-up and replaced with plastic fittings and media was manually changed daily, as the valves did not adequately submerge the scaffolds in media and affected pressure generation. Often times, these valves would allow half of the main chamber to be filled with media, with some media trapped inside the valves, and leave the scaffolds in the main chamber uncovered.

There was only one chamber for housing the scaffolds, with a maximum space for 4 samples, which limited the schedule and time-efficiency of the experiment as trials had to be performed one at a time to maintain sterility as opposed to simultaneously. For instance, if there were 2 chambers each housing 2 sets of samples, one session of 3 hour cyclic hydrostatic loading could be performed on 1 set of samples in the morning and another session of loading could be performed in the afternoon on the second set of samples. Alternatively, a chamber with a capacity for housing different and greater number of samples, i.e. individual removable units each with more than 4 spaces, would allow for more samples to be subject to cyclic loading at one time.

Sterility was also an issue with the design of this chamber. Although all individual components of the hydrostatic pressure chamber were autoclaved before housing the scaffolds, when subject to cyclic hydrostatic loading, the pressure generation fitting, which cannot be autoclaved, was threaded into the mid-chamber, possibly compromising sterility of the mid and main chamber contents. The pressure generation fitting itself was connected through tubing to a pressure sensor and pressure generation cylinder and as this unit contained silicone fluid, could not be dismantled without seeping silicone fluid. Due to the inability to remove the pressure sensor from this unit without leakage issues and the inability autoclave the pressure sensor, this unit could not be autoclaved to ensure sterility. If the unit was dismantled, silicone fluid leaked and pressure generation issues such as erratic and inconsistent pressure generation ensued. The pressure generation fitting was attached to applying cyclic hydrostatic loading and when the loading was completed, the chamber housing the cells was replaced in the

incubator until hydrostatic loading was repeated the following day or when scaffolds were removed to be imaged. It was likely the sterility of the chamber and contents was compromised in through the application of cyclic hydrostatic pressure.

Pressure generation was also a problem with the design of this chamber. Although the cyclic hydrostatic pressure applied to the samples analyzed in this research received consistent pressure, the time and effort it took to set-up the hydrostatic pressure system for each experiment was variable. Pre-loading trials ranged widely in set-up time where some experiments were ready to run at the appropriate pressure and frequency within 5-10 minutes of pre-trial loading while other experiments took as long as an hour before sufficient pressure was generated in pre-trial loading cycles. The inconsistency in pressure generation was suspected to be a result of inadequate interfacing in the chamber and pressure generation design and leakage issues within the pressure generation tubing and connections.

Air getting into the system was a consistent an issue and affected pressure generation. During experiments when no air bubbles were apparent at the beginning of a loading session, air bubbles would be observed and accumulate as the experiment progressed, becoming very apparent by the end of the experiment. Pressure generation challenges as a result of air between the pressure generation fitting and the media in the mid-chamber was also experienced. The pressure generation fitting comprised of a stainless steel segment and ring that sandwiched a piece of silicone. The piece of silicone acted as a physical block and prevented the silicone fluid from mixing with the media in

the mid-chamber. When the actuator displaced the pressure generation cylinder, the silicone fluid within the tubing was forced toward the pressure generation fitting and rendered the piece of silicone in the pressure generation fitting from a slightly concave arrangement to a convex protrusion. When no pressure was generated, the piece of silicone was in a concave arrangement and this concavity was a factor when filling the mid-chamber space since the media and the concave shape of the silicone did not match up and created air pockets, which affected pressure generation. For instance, when the pressure generation fitting was threaded into the mid-chamber and secured, the mid-chamber was filled with media through 2 individual ports on either side of the mid-chamber via a thin 18-gauge needle. The majority of the time, this method did not sufficiently fill up the mid-chamber and resulted in a lower pressure than the pressure level needed for the experiment. Additionally, in order to check whether the mid-chamber cavity was sufficiently filled, the pressure generation fitting needed be unthreaded from the mid-chamber as components were made from stainless steel with no transparent windows. When the pressure generation fitting was removed and there was a sufficient level of media, one has to carefully rethread the pressure generation fitting back into the mid-chamber without unsettling the media. When the pressure generation fitting was removed and there was not a sufficient level of media in the mid-chamber, media needed to be meticulously topped up via an 18 gauge needle and the pressure generation fitting needed to be carefully rethreaded to minimize any disturbance to the media.

When air bubbles accumulated to the point where pressure level was not sufficient, the system was bled and refilled with silicone fluid. This scenario was a

regular occurrence and impacted the cyclic loading schedule as bleeding and refilling the system and resetting the experimental setup was extremely finicky and could take up to a few hours before sufficient pressure could be generated.

5.6 Cyclic Hydrostatic Pressure

Research has demonstrated an anabolic effect of hydrostatic pressure on cell metabolism via a variety of cell sources and at a wide range of pressures and times. Handa and others observed PG synthesis in the IVD with the application of physiologically appropriate level hydrostatic pressure (3 atm) and Ishihara and others observed stimulation of ECM in NP cells when subjected to 2.5MPa of hydrostatic pressure [19, 97]. Neidlinger-Wilke and others also demonstrated similar results where hydrostatic pressure between 0.25-2.5MPa had a tendency to induce anabolic effects in IVD cells [98]. The IVD is constantly subject to loading and unloading and a NP regenerative therapy needs to account for this. The decision for subjecting the NP-seeded scaffolds to cyclic hydrostatic pressure loading at 1MPa at 1Hz for 3 hours a day for 3 days was decided upon as it was a conservative treatment that was within the range of hydrostatic loading conditions reported in relevant studies where hydrostatic loading influenced disc synthesis. Pressure at 1MPa was also consistent with intradiscal pressure values reported for typical daily human movements such as standing and bending [99], which any regenerative NP therapy should have the ability to adequately support. In this work, NP-seeded scaffolds were subjected to cyclic hydrostatic pressure loading at physiologically relevant conditions and contrary to the anabolic effects in the research mentioned above, a decreased trend in cell viability was observed. This may have

resulted from a variety of reasons including cell source, sterility issues and hydrostatic pressure chamber design as mentioned previously. Further studies utilizing alternate cell sources or a more appropriately designed hydrostatic loading device may provide a better measure toward the efficacy of a 3:1 TMHA/ELP hydrogel as a scaffold for NP tissue engineering.

5.7 Design Considerations

From relevant experience working with the custom-made hydrostatic pressure system in this research, some suggestions are recommended for future hydrostatic pressure system design.

1. Incorporate translucent windows into the chamber housing the seeded scaffolds to ensure scaffolds are correctly situated and sufficiently covered with media.
2. Design an instrument that can conveniently be put into/taken out of the chamber that securely contains the scaffolds while minimizing any impediments for ensuring sufficient hydrostatic pressure.
3. Allow for a greater number of samples to be loaded at once to enhance sample size for each trial.
4. Incorporate greater sterility measures in chamber design so scaffolds and media in the chamber are in a sterile environment at all times.
5. Integrate feedback loop in pressure loading setup to ensure consistent application of pressure.

5.8 Cell Viability

High cell viability was observed in both NP-seeded TMHA and 3:1 TMHA/ELP hydrogels at day 0 with a slight decrease in day 4 unloaded hydrogels. This was not surprising and is consistent with research by Windisch and by Moss where NP-seeded cells were cultured for up to 14 and 21 days respectively with a decrease in cell viability observed over time [90, 91]. The first trial in each of the day 4 unloaded treatments at each ratio (TMHA and 3:1 TMHA/ELP) showed a greater decrease in cell viability when compared to the results from the second and third trial in the same treatment group at the same hydrogel ratio. Due to the small sample size, it was hard to conclusively say whether this result was an outlier or if the other 2 trials were anomalies. Differing cell sources and distinct cell behaviour may have affected this outcome as both of these samples were taken from separate patients and previous research has demonstrated differences in gene expression in IVD cells from different donors [93].

The day 4 hydrostatically loaded treatment groups in both ratios demonstrated a decreasing trend in cell viability, with statistically significant differences observed between the TMHA-Day 0 unloaded treatment and the TMHA-Day 4 loaded treatment and the TMHA-Day 0 unloaded treatment and the 3:1 TMHA/ELP-Day 4 loaded treatment. This was inconsistent with studies that have applied hydrostatic loads to cells and observed increased metabolism [19, 97, 98], although the combined factors of using cells obtained from patients undergoing disc degeneration that may have been compromised to begin with and sterility and pressure generation issues associated with the hydrostatic pressure system may have influenced the result. Differences in hydrostatic loading method may also have affected cell viability as the method

undertaken in this research was carried out by a custom-made hydrostatic pressure system that was remarkably different from previous methods investigated and difficult to compare. The systems utilized by Handa and others and Neidlinger-Wilke and others took into account sterility concerns with a sterile syringe containing the samples and sterile bags with cell-loaded gels respectively [19, 98]. Given the circumstances surrounding cell source and hydrostatic loading factors, it was not perplexing to have observed a significant decrease in NP cell viability.

The similarities between NP cell viability in both TMHA and 3:1 TMHA/ELP ratios and at each treatment level seem to indicate roughly equal ability of the two ratios as a scaffold for supporting NP cells. This finding was not unanticipated in the sense that cyclic loading was applied on cells obtained from degenerate discs and the possibility was likely that these cells may not have been healthy enough to support such loading. It is interesting to note that the 3:1 TMHA/ELP hydrogel and the TMHA hydrogel demonstrated relatively similar ability to support NP seeded cells prior to and after cyclic hydrostatic pressure application even though the 3:1 TMHA/ELP hydrogel had the advantage of resiliency and elastin recoil from the addition of elastin-like polypeptides. This finding is similar to previous work by Moss and Windisch where TMHA/ELP and TMHA hydrogel formulations demonstrated similar capacity for supporting NP cells when hydrostatic pressure was not applied to the cell-seeded hydrogel scaffolds [90. 91].

5.9 Live/Dead Staining and Microscopy

Assessing cell viability via live/dead staining and microscopy imaging is a common practice that has been successfully utilized to visualize cell viability, however, there was some limitation to using this method in this research. The cells were encapsulated in hydrogels and housed for 4 days in mesh inserts contained in the hydrostatic pressure chamber. When the gels are initially encapsulated, they are made in borosilicate chamber wells (as a mold), left to gel, and then transferred to mesh inserts and placed in the hydrostatic chamber. When the scaffolds are imaged, they are removed from the mesh inserts and transferred back into wells of a borosilicate chamber. The transfer of scaffolds from the initial borosilicate chamber wells to the mesh inserts and back into the borosilicate chamber wells tended to result in hydrogel loss and altered the structure of the hydrogel and this manhandling may have affected cell viability and imaging results.

The live/dead staining of the cells pose another concern as a method for assessing cell viability. In this research, the NP cells did fluoresce when visualized under the microscope, but the live/dead stain did not completely penetrate all cells in the scaffold. The amount of cells observed under white light was greater than the amount of cells that eventually fluoresced. This could have been a result of stain diffusion time or inability of the stain to completely penetrate the scaffold and may have affected accuracy in cell viability assessment.

Though the use of [3H]-thymidine to measure incorporation into the DNA of cultured cells and terazolium salt assay to assess cell proliferation and viability offer

alternate methods of quantifying cell proliferation [100, 101], there is does not seem to be a method that provides a perfect application for this research as the crosslinkages in the hydrogels may present an issue.

5.10 Gene Analysis Limitations

Results from RT-PCR offer information about the efficacy and effect of cyclic loading on NP cell gene expression. For all samples, the expression of the 2 housekeeping genes, GAPDH and 18s, indicated regulation in cell function and acted sufficiently to control for error between samples. The lack of relevant NP gene expression in the majority of the samples suggested that the NP phenotype was not adequately maintained. Aggrecan, collagen type I and collagen type II are important NP ECM molecules and their absence in the majority of all samples regardless of ratio or treatment group indicates a lack of NP phenotypic maintenance. Though this result would not have been as surprising in the day 4 loaded samples, it is interesting that the majority of all samples, regardless or ratio or treatment group, did not express any genes besides the GAPDH and 18s. This finding suggests that the cells were compromised as the absence of SOX9 in almost all samples is indicative of IVD degeneration as SOX9 is a transcription factor responsible for chrondrogenesis and an important driver of the NP phenotype [17]. As the expression of SOX9 is decreased with degeneration of the IVD, it is not startling to find a lack of SOX9 expression.

The control, which contained NP cells cultured in monolayer that was not encapsulated or subject to pressure loading, only expressed collagen type II in addition to

the 2 housekeeping genes. This finding is contrary to the results observed by Yang and others where gene analysis of NP cell-seeded scaffolds showed higher type II collagen and aggrecan expression than cells cultured in monolayer [102]. The collagen type II expression observed in this result may be attributed to cell source and properties from the sample donor.

CD24 expression was only apparent in one sample out of all ratios and treatment groups and this may again be attributed to variations in donor properties as this particular sample was obtained from a young female patient (born: 1981; youngest patient whose disc sample was obtained for this research), potentially indicating less degeneration or greater NP-phenotype maintenance ability although this is inconsistent with findings by Fujita and others who were able to detect CD24 expression in herniated NP and chordoma, but not in chondrosarcoma cells, indicating CD24 as a molecular for the NP even in diseased samples [16]. It is interesting to note that CD24 gene expression was absent in the majority of samples, though when analyzed via flow cytometry, the CD24 marker was present in all samples used for encapsulation. The possibility exists that between flow cytometry and encapsulation, the NP cells sheds this marker or that there are limitations from the RT-PCR findings. A more qualitative gene expression analysis technique, such as realtime PCR may offer more insight into the expression of NP-seeded scaffolds.

The expression of collagen type I and collagen type II in 2 individual samples may also be attributed to variations in donor cell properties as the expression occurred at such a low frequency and in a minority of samples.

Chapter 6 Conclusions

6.1 Summary of Relevant Findings

The main goal of this research was to evaluate the potential of a 3:1 TMHA/ELP composite hydrogel as an effective scaffold for NP tissue engineering for application in early-stage IVD degeneration. The criteria for this scaffold must consider the cyclic hydrostatic pressure loading and unloading experienced by cells in the IVD and must be biocompatible. The scaffold must also be easy to handle and feasible if clinical application is to be successful and the scaffold must also sufficiently support cell viability, encourage cell proliferation and maintain the NP phenotype. The 3:1 TMHA/ELP hydrogel was evaluated under these considerations.

In vitro work demonstrated the 3:1 TMHA/ELP hydrogel produced a viable environment for the cultured NP cells as cell viability in unloaded treatment groups at day 0 and 4 demonstrated a high percentage of live cells when compared to dead cells. As well, the cells cultured in monolayer took on a thin, spindle-like morphology but reverted into a spherical, chondrocyte-like morphology characteristic of NP cells when encapsulated, suggesting potential of the 3:1 TMHA/ELP hydrogel as a relevant biological scaffold. The NP cells were evenly distributed within in the 3:1 TMHA/ELP scaffold and were quick to cure *in situ,* crosslinking within a few minutes upon the addition of PEGDA. When cyclic hydrostatic loading was applied to the NP-seeded scaffold, cell viability drastically decreased, suggesting that either the cells could not handle the mechanical stress as they were obtained from a compromised source, or the scaffold was inadequate in creating a biologically relevant environment capable of

supporting NP cells, or challenges associated with pressure generation (i.e. inconsistent pressure generation, sterility issues) negatively affected cell function. Gene expression analysis via RT-PCR also indicated a lack of relevant NP ECM gene expression and this may have been a result of cell source or hydrostatic pressure challenges or highlights a need for a more qualitative gene expression analysis technique. The possibility of compromised NP cells obtained from a degenerate cell source and problematic hydrostatic pressure loading methods are likely to have impacted these results.

6.2 Conclusions

TMHA and ELP are biologically relevant biomaterials that have the potential to provide an adequate scaffold for NP tissue engineering. Cell viability and chondrocyte-like NP morphology was maintained in NP-seeded 3:1 TMHA/ELP hydrogel scaffolds during the course of 4 days, and even distribution of NP cells and rapid curing time *in situ* demonstrated feasibility of the scaffold as a vehicle for a relatively non-invasive injectable therapy. While the findings from this research show a decrease in cell viability after the application of cyclic hydrostatic loading and unloading and a lack of relevant NP gene expression after a 4-day period, it is likely that cell source and hydrostatic pressure loading method may have affected this outcome. This work is relevant to ongoing studies in NP tissue engineering as it is one of the few studies to apply cyclic hydrostatic pressure to cell-seeded scaffolds and contributes to an understanding of what was and was not viable, offering insight for further research. Further investigation using alternate cell type and a more consistent and sterile pressure system may provide better insight into the evaluation of a 3:1 TMHA/ELP hydrogel for nucleus pulposus tissue engineering.

6.3 Future Work

1. Cells to be encapsulated in the TMHA-based hydrogels should be of a healthy and consistent source to offer more control and minimize variability for a more accurate assessment of the hydrogel.
2. Sample sizes and trial repetitions should be increased in order to draw more conclusive findings.
3. The live/dead stain was problematic since not all cells stained fluoresced possibly due to inadequacy of the stain to permeate the scaffold. Alternate methods of assessing cell viability in a more quantifiable method might provide a more accurate evaluation of cell viability.
4. A revised method for applying hydrostatic pressure should be undertaken to minimize hydrogel handling and sterility issues to provide a system that offers more control and consistency when applying hydrostatic pressure.
5. Quantitative PCR should be undertaken to ascertain between levels of gene expression between the TMHA and 3:1 TMHA/ELP hydrogels ratios and clarify understanding regarding the addition of ELP in the scaffold and any effect this may have.

References

1. Levin, D.A., Bendo, J.A., Quirno, M., Errico, T., Goldstein, J. and J. Spivak. 2007. Comparative charge analysis of one- and two-level lumbar total disc arthroplasty versus circumferential lumbar fusion. *Spine* 32(25): 2905-2909.
2. Roughley, P. 2004. Biology of the intervertebral disc aging and degeneration: involvement of the extracellular matrix. *Spine* 29(23): 2691-2699.
3. Waddell, G. 1996. Low back pain: A twentieth century health care enigma. *Spine* 21: 2820-2825.
4. Dagenais, S., Caro, J. and S. Haldeman. 2008. A systematic review of low back pain cost of illness studies in the United States and internationally. *Spine J* 8: 8-20.
5. Abenhaim, L., Suissa, S. and M. Rossignol. 1988. Risk of recurrence of occupational back pain over three-year follow-up. *Br J Ind Med* 45(12): 829-833.
6. Rossignol, M., Suissa, S. and L. Abenhaim. 1988. Working disability due to occupational back pain: three-year follow-up of 2300 compensated workers in Quebec. *J Occup Med* 30(6): 502-505.
7. Gray, H. 2008. *Gray's Anatomy: The Anatomical Basis of Medicine and Surgery, 40th edition*. Edinburgh, UK: Churchill-Livingstone, Elsevier.
8. Clemente, C.D. 2007. *Anatomy: a regional atlas of the human body, 5th edition.* Maryland, USA: Lippincott, Williams and Wilkins.
9. Bao, Q.B., McCullen, G.M., Higham, P.A., Dumbleton, J.H. and H.A. Yuan. 1996. The artificial disc: theory, design and materials. *Biomaterials* 17(12): 1157-1167.
10. O'Halloran, D.M. and A.S. Pandit. 2007. Tissue engineering approach to regenerating the intervertebral disc. *Tissue Eng* 13(8): 1927-1954.
11. Roberts, S., Evans, H., Trivedi, J. and J. Menage. 2006. Histology and pathology of the human intervertebral disc. *J Bone Joint Surg Am* 88(2): 10-14.
12. Adams, M.A. and P.J. Roughley. 2006. What is intervertebral disc degeneration and what causes it? *Spine* 31(18): 2151-2161.
13. Ghosh, P., Bushell, G.K., Taylor, T.F.K. and W.H. Akeson. 1977. Collagen, elastin and noncollagenous protein of the intervertebral disc. *Clin Orthop* 129: 124-132.
14. Antoniou, J., Steffen, T., Nelson, F., Winterbottom, N., Hollander, A.P., Poole, R.A., Aebi, M. and M. Alini. 1996. The human lumbar intervertebral disc: evidence for changes in the biosynthesis and denaturation of the extracelluar matrix with growth, maturation, ageing and degeneration. *J Clin Invest* 98(4): 996-1003.
15. Sive, J.I., Baird, M., Jeziorsk, A., Watkins, Hoyland, J.A. and A.J. Freemont. 2002. Expression of chondrocyte markers by cells of normal and degenerate intervertebral discs. *Mol Path* 55(2): 91-97.
16. Fujita, N., Miyamoto, T., Imai, J-I., Hosogane, N., Suzuki, T., Yagi, M., Morita, K., Ninomiya, K., Miyamoto, K., Takaishi, H., Matsumoto, M., Morioka, H., Yabe, H., Chiba, K., Watanabe, S., Toyama, Y. and T. Suda. 2005. CD24 is expressed specifically in the nucleus pulposus of intervertebral discs. *Biochem Biophys Res Comm* 338(4): 1890-1896.
17. Hering TM. 1999. Regulation of chondrocyte gene expression. *Front Biosci* 4:743-61.
18. Altman, G.H., Horan, R.L., Martin, I., Farhadi, J., Stark, P.R.H., Volloch, V., Richmond, J.C., Vunjak-Novakovic, G. and D.L. Kaplan. 2001. Cell differentiation by mechanical stress. *FASEB Journal* 16: 270-272.
19. Handa, T., Ishihara, H., Ohshima, H., Osada, R., Tsuji, H. and K. Obata. 1997. Effects of hydrostatic pressure on matrix synthesis and matrix metalloproteinase production in the human lumbar intervertebral disc. *Spine* 22(10): 1085-1091.
20. Angele, P., Yo, J.U., Smith, C., Mansour, J., Jepsen, K.J., Nerlich, M. and B. Johnstone. 2003. Cyclic hydrostatic pressure enhances the chondrogenic phenotype of human mesenchymal progenitor cells differentiated in vitro. *J Orthpo Res* 21(3): 451-457.
21. Hall, A.C., Urban, J.P.G. and K.A. Gehl. 1991. The effects of hydrostatic pressure on matrix synthesis in articular cartilage. *J Orthop Res* 9(1): 1-10.

22. Smith, R.L., Rusk, S.F., Ellison, B.E., Wessells, P., Tsuchiya, K., Carter, D.R., Caler, W.E., Sandell, L.J. and D.J. Schurman. 1996. In vitro stimulation of articular chondrocytic mRNA and extracellular matrix synthesis by hydrostatic pressure. *J Orthop Res* 14(1): 53-60.
23. Tow, B.P.B., Hsu,W.K., and J.C. Wang. 2007. Disc Regeneration: A Glimpse of the Future *Clin Neurosurg* 54: 122-128.
24. Cassidy, J., Hiltner, A. and E. Baer. 1990. The response of the hierarchical structure of the intervertebral disc to uniaxial compression. *J Mat Sci: Mat Med* 1: 69-80.
25. Roughley, P., Hoemann, C., DesRosiers, E., Mwale, F., Antoniou, J. and M. Alini. 2006. The potential of chitosan-based gels containing intervertebral disc cells for nucleus pulposus supplementation. *Biomaterials* 27(3): 388-396.
26. Alini, M., Li, W., Markovic, P., Aebi, M., Spiro, R.C. and P.J. Roughley. 2003. The potential and limitations of a cell-seeded collagen/hyaluronan scaffold to engineer an intervertebral disc-like matrix. *Spine* 28(5): 446-454.
27. An, H.S. and K. Masuda. 2006. Relevance of in vitro and in vivo models for intervertebral disc degeneration. *J Bone Joint Surg Am* 88(S2): 88-94.
28. Goins, M.L., Wimberley, D.W., Yuan, P.S., Fitzhenry, L. and A.R. Vaccaro. 2005. Nucleus pulposus replacement: an emerging technology. *Spine J* 5(6S): 317-324.
29. Whang, P.G. and J.C. Wang. 2003. Bone graft substitutes for spinal fusion. *Spine* 3(2): 155-165.
30. Depuy Spine Inc. 2009. Charite® artificial disc. Retrieved March 18 2009, from http://www.charitedisc.com/charitedev/domestic/
31. DePuy Spine Inc. 2010. DePuy Product Catalogy. Retrieved December 21 2010, from http://www.depuy.com/healthcare-professionals/products-list/
32. Mathiesen, E.B., Lindgren, J.U., Reinholt, F.P. and E. Sudmann. 2004. Tissue reactions to wear products from polyacetal (Delrin®) and UHMW polyethylene in total hip replacement. *J Biomed Mat Res* 21: 459-466.
33. Van Ooji, A., Kurtz, S.M., Stessels, F., Noten, H. and L. van Rhijn. 2007. Polyethylene wear devris and long-term clinical failure of the Charite disc prothesis. *Spine* 32(2): 223-229.
34. Nachemson, A. 1962. Some mechanical properties of the lumbar intervertebral disc. *Bull Hasp Joint Dis* 23: 130-132.
35. Ray, C.D.1991. *Lumbar interbody threaded prostheses.* Berlin, Heidelberg, New York: Springer.
36. Ray, C.D. 2002. The PDN® prosthetic disc-nucleus device. *Eur Spine J* 11(S2): 137-142
37. Yu, S., Haughton, V.M., Ho, P.S., Sether, L.A., Wagner, M. and K.C. Ho. 1988. Progressive and regressive changes in the nucleus pulposus. II. The adult. *Radiology* 169: 93–97.
38. Shim, C.S., Lee, S.H., Park, C.W., Choi, W.C., Choi, G., Choi, W.G, Lim, S.R. and H.Y. Lee. 2003. Partial disc replacement with the PDN prosthetic disc nucleus device: early clinical results. *J Spinal Disord Tech* 16(4): 324-330.
39. Coric, D. and P.V. Mummaneni. 2008. Nucleus replacement technologies. *J Neurosurg Spine* 8(2): 115-120.
40. Griffith, S.L., Shelokov, A.P., Buttner-Janz, K., LeMaire, J.P. and W.S. Zeegers. 1994. A multicenter retrospective study of the clinical results of the LINK SB Charite intervertebral prosthesis. *Spine* 19: 1842-1949.
41. McAfee, P.C., Geisler, F.H., Saiedy, S.S., Moore, S.V., Regan, JJ., Guyder, R.D., Blumenthal, S.L., Fedder, I.L., Tortolani, P.J. and B. Cunningham. 2006. Revisability of the CHARITE artificial disc replacement. *Spine* 11: 1217-1226.
42. Wakatsuki, T. and E.L. Elson. 2003. Reciprocal interactions between cells and extracellular matrix during remodeling of tissue constructs. *Biophys Chem* 100: 593-605.
43. Gruber, H.E., and E.N.Hanley Jr. 2003. Biologic strategies for the therapy of intervertebral disc degeneration. *Expert Opin Biol Ther* 3: 1209-1214.
44. Guoping, C., Takashi, U. and T. Tateishi. 2002. Scaffold design for tissue engineering. *Macromol Biosci* 2: 67-77.
45. Williams, D.F. 2008. On the mechanisms of biocompatibility. *Biomaterials* 29(20): 2941-2953.
46. Chen, G., Ushida, T. and T. Tateishi. 2002. Scaffold design for tissue engineering. *Macromol Biosci* 2(2):67-77.
47. Anderson, G., Risbud, M.V., Shapiro, I.V., Vaccaro, A. and T.J. Albert. 2005. Cell-based therapy for disc repair. *Spine J* 5(S6): 297-393.
48. Hoffman, A.S. 2002. Hydrogels for biomedical applications. *Adv Drug Deliv Rev* 54(1): 3-12.

49. Boyd, L.M. and A.J. Carter. 2006. Injectable biomaterials and vertebral endplate treatment for repair and regeneration of the intervertebral disc. *Eur Spine J* 15(S3): S414-S421.
50. Temenoff, J.S. and A.G. Mikos. 2000. Injectable biodegradable materials for orthopedic tissue engineering. *Biomaterials* 21(23): 2405-2412.
51. Girish, K.S. and K. Kemparaju. 2007. The magic glue hyaluronan and its eraser hyaluronidase: a biological overview. *Life Sci* 80(21): 1921-43.
52. Laurent, T.C. and J.R. Fraser. 1992. Hyaluronan. *Faseb J.* 6(7): 2397-2404.
53. Vercruysse, K.P., Marecak, D.M., Marecek, F. and G.D. Prestwich. 1997. Synthesis and in vitro degradation of new polyvalent hydrazide crosslinked hydrogels of hyaluronic acid. *Bioconjug Chem* 8(5): 686-694.
54. Wight, T.N., Kinsella, M.G. and E.E. Qwarnstrom. 1992. The role of proteoglycans in cell adhesion, migration and proliferation. *Cur Opinion Cell Biol* 4: 793-801.
55. Bastow, E.R., Byers, S., Golub, S.B., Clarkin, C.E., Pitsillides, A.A. and A. J. Fosang. 2008. Hyaluronan synthesis and degradation in cartilage and bone. *Cell Mol Life Sci* 65(3): 395-413.
56. Shu, X. Z., Liu, Y.C., Luo, Y., Roberts, M.C. and G.D. Prestwich. 2002. Disulfide cross-linked hyaluronan hydrogels. *Biomacromolecules* 3(6): 1304-1311.
57. Serban, M.A. and G.D. Prestwich. 2007. Synthesis of hyaluronan haloacetates and biology of novel crosslinker-free synthetic extracelluar matrix hydrogels. *Biomacromolecules* 8(9): 2821-2828.
58. Shu, X.S., Liu, Y., Palumbo, F.S., Luo, Y. and G.D. Prestwich. 2004. In situ crosslinkable hyaluronan hydrogels for tissue engineering. *Biomaterials* 25(7-8): 1339-1348.
59. Xiao, Z.S., Liu, Y.C., Palumbo, F.S., Luo, Y. and G.D. Prestwich. 2004. In situ crosslinkable hyaluronan hydrogels for tissue engineering. *Biomaterials* 25(7-8): 1339-1348.
60. Liu, Y., Zheng, S. X. and G.D. Prestwich. 2005. Biocompatibility and stability of disulfide-crosslinked hyaluronan films. *Biomaterials* 26(23): 4737-4746.
61. Ghosh, K., Shu, X.Z., Mou, R., Lombardi, J., Prestwich, G.D., Rafailovich, M.H. and R.A.F. Clark. 2005. Rheological characterization of in situ cross-linkable hyaluronan hydrogels. *Biomacromolecules* 6(5): 2857-2865.
62. Park, A.H., Hughes, C.W., Jackson, A., Hunter, L., McGill, L., Simonsen, S.E., Alder, S.C., Shu, X.Z. and G.D. Prestwich. 2006. Crosslinked hydrogels for tympanic membrane repair. *Otolaryngol Head Neck Surg* 135(6): 877-883.
63. Liu, Y., Shu., X.Z. and G.D. Prestwich. 2007. Reduced postoperative intra-abdominal adhesions using Carbylan-SX, a semisynthetic glycosaminoglycan hydrogel. *Fertil Steril* 87(4): 940-948.
64. Segura, T., Anderson, B.C., Chung, P.H., Webber, R.E., Shull, K.R. and L.D. Shea. 2005. Crosslinked hyaluronic acid hydrogels: a strategy to functionalize and pattern. *Biomaterials* 26(4): 359-371.
65. Stern, S., Lindenhayn, K., Schultz, O. and C. Perka. 2000. Cultivation of porcine cells from the nucleus pulposus in a fibrin/hyaluronic acid matrix. *Acta Orthop Scand* 71(5): 496-502.
66. Pfiffer, M., Boudroit, U., Pfeiffer, D., Ishaque, N., Goetz, W., and A. Wilke. 2003. Intradiscal application of hyaluronic acid in the non-human primate lumbar spine: radiological results. *Euro Spine J.* 12(1): 76-83.
67. Crevensten, G., Walsh, A.J.L., Ananthakrishnan, D., Page, P., Wahba, G.M., Lotz, J.C. and S. Berven. 2004. Intervertebral disc cell therapy for regeneration: mesenchymal stem cell implantation in rat intervertebral discs. *Ann Biomed Eng* 32(3): 430-434.
68. Halloran, D.O., Grad, S., Stoddart, M., Dockery, P., Alini, M. and A. S. Pandit. 2008. An injectable crosslinked scaffold for nucleus pulposus regeneration. *Biomaterials* 29(4): 438-447.
69. Vrhovski, B. and A.S. Weiss. 1998. Biochemistry of tropoelastin. *Eur J Biochem* 258(1): 1-18.
70. Mecham, R. and E. Davis. 1994. *Elastic fibre structure and assembly.* San Diego, USA: Academic Press.
71. Keeley, F.W., Bellingham, C.M. and K.A. Woodhouse. 2002. Elastin as a self-organizing biomaterial: use of recombinantly expressed human elastin polypeptides as a model for investigations of structure and self-assembly of elastin. *Philos Trans R Soc Lond B Biol Sci* 357(1418): 185-189.
72. Karnik, S.K., Brooke, B.S., Bayes-Genis, A., Sorensen, L., Wythe, J.D., Schwartz, R.S., Keating, M.T. and D.Y. Li. 2002. A critical role for elastin signaling in vascular morphogenesis and disease. *Development* 130(2): 411-423.

73. Woodhouse, K.A., Kiement, P., Chen, V., Gorbet, M.B., Keeley, F.W., Stahl, R., Fromstein, J.D., Catherine, C.M. and M. Bellingham. 2004. Investigation of recombinant human elastin polypeptides as non-thrombogenic coatings. *Biomaterials* 25(19): 4543-4553.
74. Jordan, S.W., Haller, C.A., Sallach, R.E., Apkarian, R.P., Hanson, S.R. and E.L. Chaikof. 2007. The effect of a recombinant elastin-mimetic coating of an ePTFE prosthesis on acute thrombogenicity in a baboon arteriovenous shunt. *Biomaterials* 28(6): 1191-1197.
75. Herrero-Vanrell, R., 2005. Self-assembled particles of an elastin-like polymer as vehicles for controlled drug release. *J Control Release* 102(1): 113-122.
76. Betre, H., Setton, L.A., Meyer, D.E. and A. Chilkoti. 2002. Characterization of a genetically engineered elastin-like polypeptide for cartilaginour tissue repair. *Biomacromolecules* 27(1): 91-99.
77. Cloyd, J.M. and D.M. Elliott. 2007. Elastin content correlates with human disc degeneration in the annulus fibrosus and nucleus pulposus. *Spine* 32(17): 686-694.
78. Yu, J., Fairbank, J.C., Roberts, S. and J. Urban. 2005. The elastic fibre network of the annulus fibrosus of the normal and scoliotic human intervertebral disc. *Spine* 30(16): 1815-1820.
79. Smith, L.J. and N.L. Fazzalari. 2006. Regional variations in the density and arrangement of elastic fibres in the annulus fibrosus of the human lumbar disc. *J Anat* 29(3): 359-367.
80. Yu, J. 2002. Elastic tissues of the intervertebral disc. *Biochem Soc trans* 30(6): 848-852.
81. Bellingham, C.M., Lillie, M.A., Gosline, J.M., Wright, G.M., Starcher, B.C., Bailey, A.J., Woodhouse, K.A. and F.W. Keeley. 2003. Recombinant human elastin polypeptides self-assemble into biomaterials with elastin-like properties. *Biopolymers* 70(4): 445-455.
82. Bellingham, C.M., Woodhouse, K.A., Robson, P., Rothstein, S.J. and F.W. Keeley. 2001. Self-aggregation charactertistics of recombinantly expressed human elastin polypeptides. *Biochimica et Biophysica* 1550(1): 6-19.
83. Bellingham, C.M. and F.W. Keeley. 2004. Self-ordered polymerization of elastin-based biomaterials. *Current Opinion Solid State Mats Sci* 8: 135-139.
84. Urry, D. 1982. Characterization of soluble peptides of elastin by physical techniques. *Methods Enzymol* 82(A): 673-716.
85. Simnick, A.J., Lim, D.W., Chow, D. and A. Chilkoti. 2007. Biomedical and biotechnological applications of elastin-like polypeptides. *J Macromolec Sci, Part C: Polymer reviews* 47(1): 33.
86. Bidwell III, G.L., Fokt, I., Preibe, W. and D. Raucher. 2007. Development of elastin-like polypeptide for thermally targeted delivery of doxorubicin. *Biochem Pharmacol* 73(5): 620-631.
87. McHale, M.K., Setton, L.A. and A. Chilkoti. 2005. Synthesis and in vitro evaluation of enzymatically crosslinked elastin-like polypeptide gels for cartilaginous tissue repair. *Tissue Eng* 11(11-12): 1768-1769.
88. Betre, H., Ong, S.R., Guilak, F., Chilkoti, A., Fermor, B. and L.A. Setton. 2006. Chondrocytic differentiation of human adipose-derived adult stem cells in elastin-like polypeptide. *Biomaterials* 27(1): 91-99.
89. Chiba, K., Anderson, G.B., Masuda, K. and E.J. Thonar. 1997. Metabolism of the extracellular matrix formed by intervertebral disc cells cultured in alginate. *Spine* 22(24): 2885-2893.
90. Moss, I. 2008. *Modified-hyaluronan and elastin-like polypeptide composite material for tissue engineering of the nucleus pulposus.* MASc thesis. University of Toronto, Toronto, Ontario. Print.
91. Windisch, L.M. 2008. *Design and evaluation of a disulphide-crosslinked hyaluronan hydrogel for regeneration of the intervertebral disc.* University of Toronto, Toronto, Ontario. Print.
92. Sakai, D., Mochida, J., Iwashina, T., Watanabe, T., Suyama, K., Ando, K and T. Hotta. 2007. Atelocollagen for culture of human nucleus pulposus cells forming nucleus pulposus-like tissue in vitro: influence on the proliferation and proteoglycan production of HNPSV-1 cells. *Biomaterials* 7(3): 346-353.
93. Kluba, T., Niemeyer, T. and C. Gaissmaier. 2007. Human annulus fibrosis and nucleus pulposus cells of the intervertebral disc: effect of degeneration and culture system on cell phenotype *Spine* 30(24): 2743-2748
94. Aguiar, D.J., Johnson, S.L. and T. R. Oegema Jr. 1999. Notochordal cells interact with nucleus pulposus cells: regulation of proteoglycan synthesis. *Exp Cell Res* 246(1): 129-137.
95. Erwin, W.M. and R.D. Inman. 2006. Notochordal cells regulate intervertebral disc chondrocyte proteoglycan production and cell proliferation. *Spine* 31(10): 1094-1099.

96. Le Visage, C., Kim, S.W., Tateno, K., Sieber, A., Kostuik, J. and K. Leong. 2006. Interaction of human mesenchymal stem cells with disc cells: changes in biosynthesis of extracellular matrix. *Spine* 31(18): 2036-2042.
97. Ishihara, H., McNally, D.S., Urban, J.P. and A.C. Hall. 1996. Effects of hydrostatic pressure on matrix synthesis in different regions of the intervertebral disk. *J Appl Physiol* 80(3): 839-846.
98. Neidlinger-Wilke, C., Wurtz, K., Urban, J.P.G., Borm, W., Arand, M., Ignatius, A., Wilke, H-J. and L.E. Claes. 2006. Regulation of gene expression in intervertebral disc cells by low and high hydrostatic pressure. *Eur Spine J*. 15(S3): 372-378.
99. Wilke, H-J., Neef, P., Caimi, M., Hoogland, T. and L.E. Claes. 1999. New in vivo measurement of pressures in the intervertebral disc in daily life. *Spine* 24(8): 755-762.
100. Gruber, H.E., Ingram, J.A., Leslie, K., Norton, H.J. and E.N. Hanley Jr. 2003. Cell shape and gene expression in human intervertebral disc cells: in vitro tissue engineering studies. *Biotech Histochem* 78(2): 109-117.
101. Leone, G., Toricelli, P., Chiumiento, A., Facchini, A. and R. Barbucci. 2008. Amidic alginate hydrogel for nucleus pulposus replacement. *J Biomed Mater Res A* 84(2): 391-401
102. Yang, S-H., Chen, P-Q., Chen, Y-F.and F-H. Lin. 2005. An in vitro study on regeneration of human nucleus pulposus by using gelatin/chondroitin-6-sulphate/hyaluronan tricopolymer scaffold. *Art Org* 29(10): 806-814

Appendix A: Hydrostatic Pressure Chamber Timeline and Issues

Hydrostatic pressure chamber timeline and issues

DATE	ACTION
July 2009	-Hydrostatic pressure (HP) chamber arrived end of this month
August 2009- September 2009	-Set-up HP system -Missing some components (threaded bits, no system to house more than 1 sample at a time, etc.) -Contacted Tissue Growth Technologies (TGT) -Had parts machined to complete HP set-up
November 2009- January 2010	-Issues with air bubbles apparent -E-mail and telephone correspondence with TGT to troubleshoot
February 2010	-Prepared HP report for TGT
March 2010 – April 2010	-Troubleshoot HP system based on feedback from TGT following their receipt of HP report
May 2010	-HP system is OK to use but very inconsistent and unstable pressure generation
June 2010- July 2010	-Loaded NP seeded samples, very inconsistent pressure generation -HP performance seemed to degrade with each use
August 2010	-HP system sent back to TGT
September 2010	-HP system sent back to OBL; broken in transit -Contacted TGT for new parts -New parts arrive end of month -Begin cyclic loading experiments

Table A1. Timeline of interactions with hydrostatic pressure chamber apparatus and hydrostatic pressure chamber issues

Appendix B: Unused Pressure Generation Trial Data

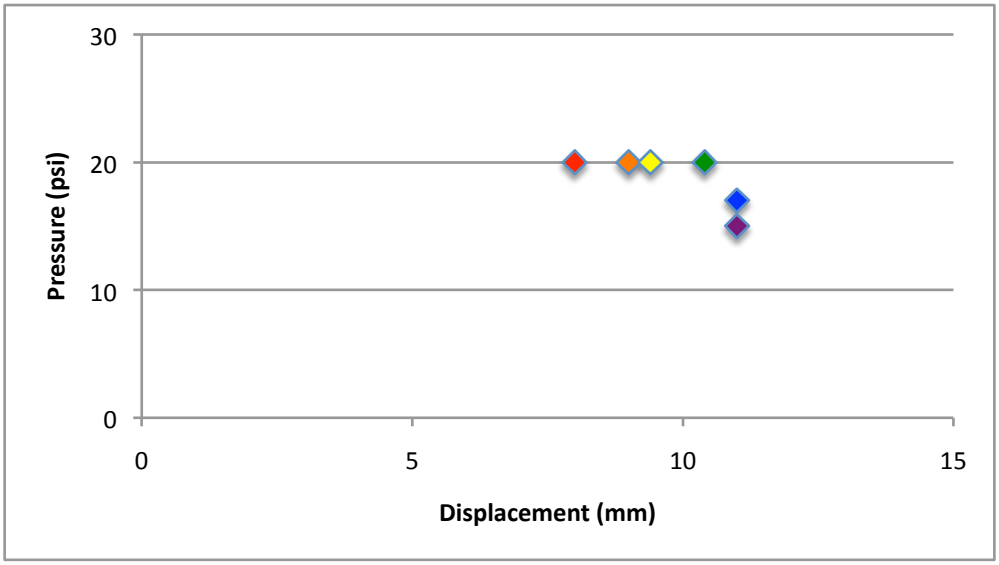

Figure B1. Pressure generated during 6 subsequent 35-second pre- trial cycles during day 1 of experimental hydrostatic pressure testing.

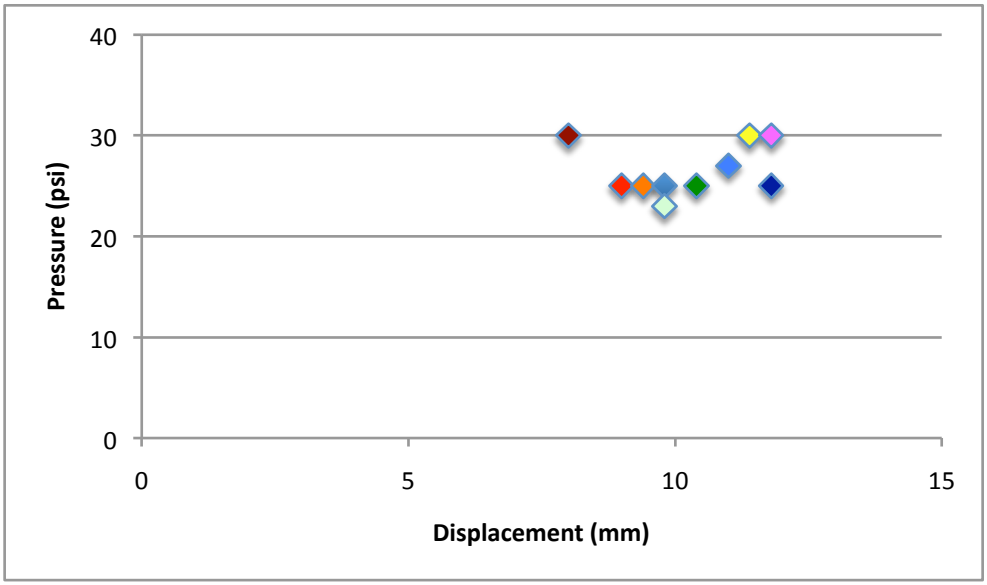

Figure B2. Pressure generated during 10 subsequent 35-second pre-trial cycles on during day 2 of experimental hydrostatic pressure testing.

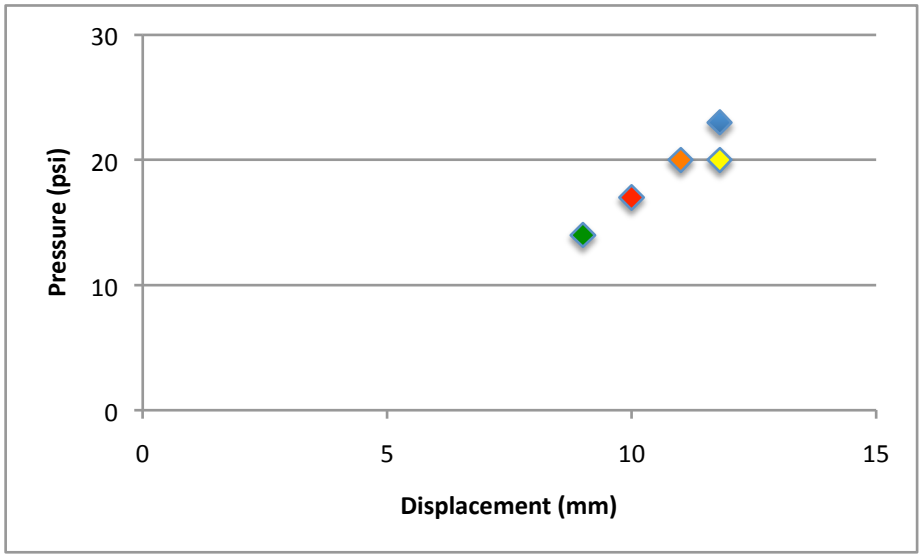

Figure B3. Pressure generated during 5 subsequent 35-second pre-trial cycles during day 3 of experimental hydrostatic pressure testing.

Appendix C: Hydrostatic Pressure Report

Tissue Growth Technologies Hydrostatic Pressure Chamber

SETTING:

Displacement control

SET-UP ISSUES:

1. Air bubbles present in the tubing connecting the pressure generator cylinder to the aluminum T-fitting, from the T-fitting to the pressure sensor and from the T-fitting to the stainless steel chamber. See image 1 and 2 below.

2. Slow fluid leakage apparent through tubing connecting the pressure generator cylinder and the aluminum T-fitting. See image 1 and 3 below.

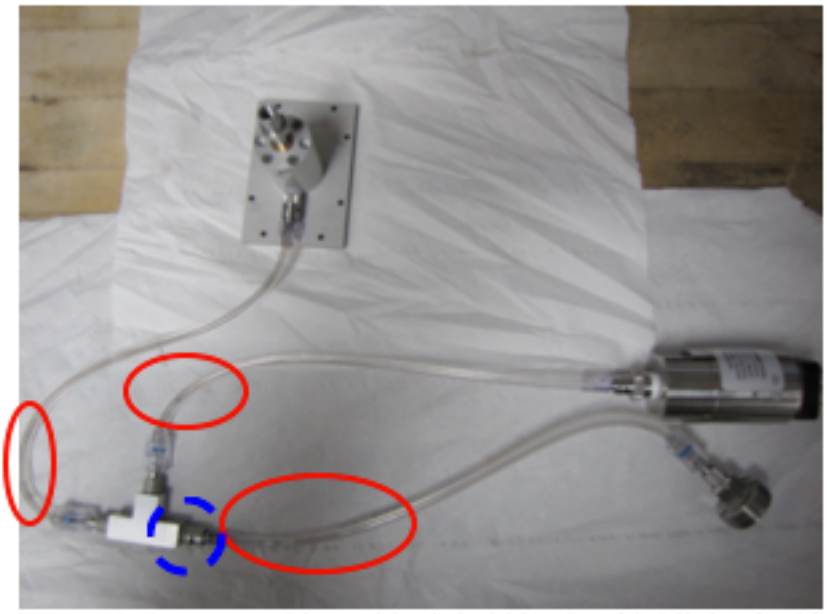

Image 1. Pressure tubing with air bubble sites highlighted with red and leak site highlighted with the blue dash line.

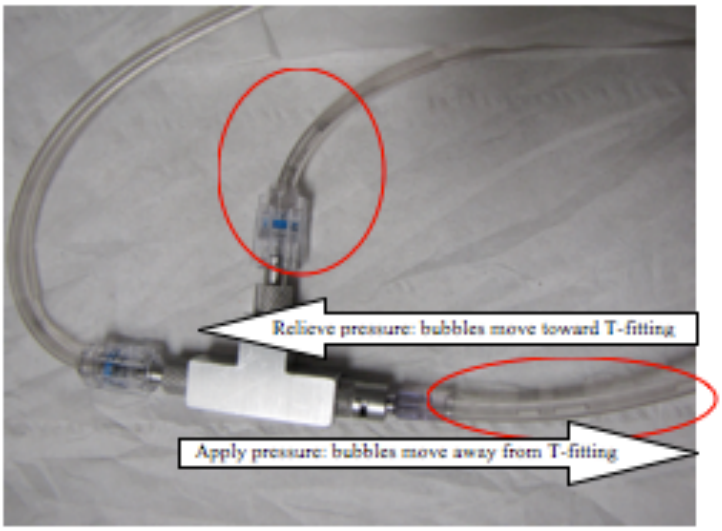

Image 2. Close-up of the air bubble sites. Air bubbles are prominent in 2 of the 3 tubing branches.

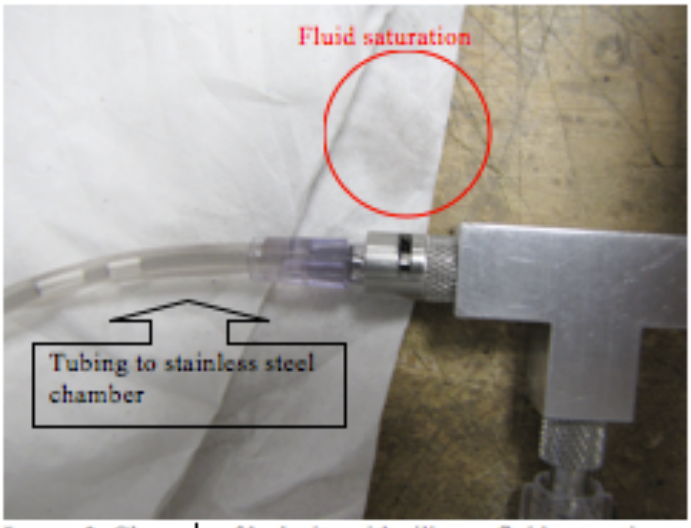

Image 3. Close-up of leak site with silicone fluid saturation apparent on the paper towel. (Paper towel was shifted northward to obtain a clearer view of the saturation).

3. Though the air bubbles and leakage have not compromised the target pressure (~145 psi), it has:

    a. Hindered the pressure generator from reaching its full limit of generating pressure up to 500 psi

    b. Created a need for the silicone fluid in the tubing needs to refilled (once bled of air bubbles) frequently (~once per week when cycles are run)

c. Created a need to replace the silicone membrane on the stainless steel chamber that connects into the mid-chamber frequently (~once per week when cycles are run) due to deformation

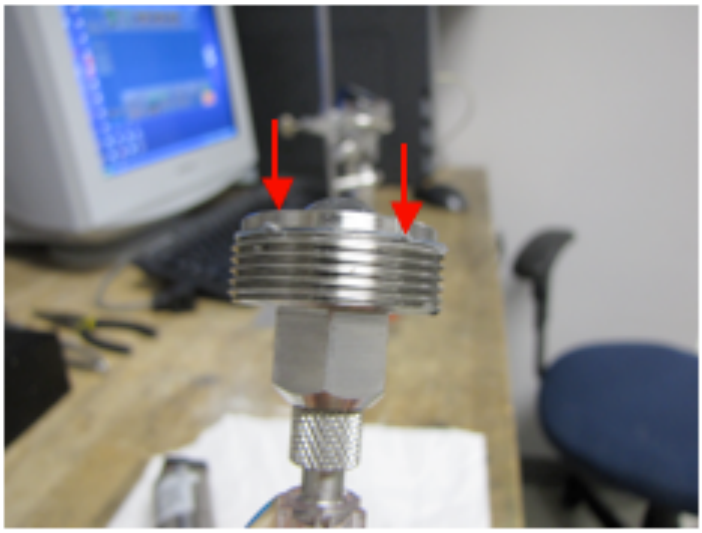

Image 4. Deformation of the silicone membrane furling up between the stainless steel ring and the steel threaded attachment of the mid-chamber.

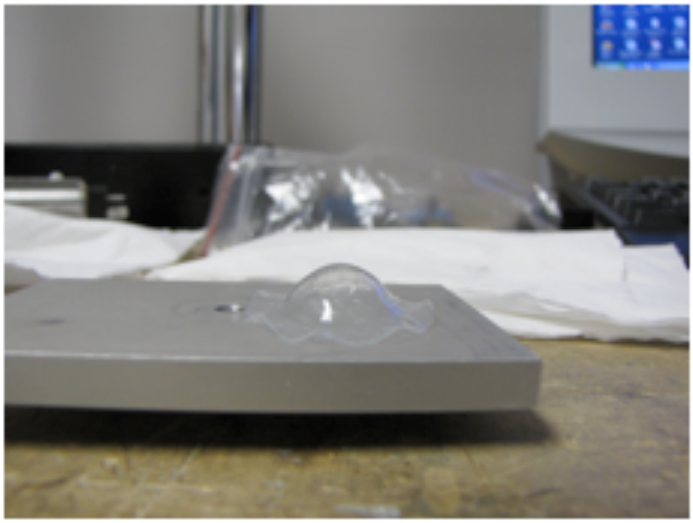

Image 5. Deformation of the silicone membrane removed from the stainless steel attachment to the mid-chamber.

PRESSURE CYCLE ISSUES:

1. In cyclic runs, the pressure and load remained fairly stable in longer trial though some instability was observed in shorter trials.

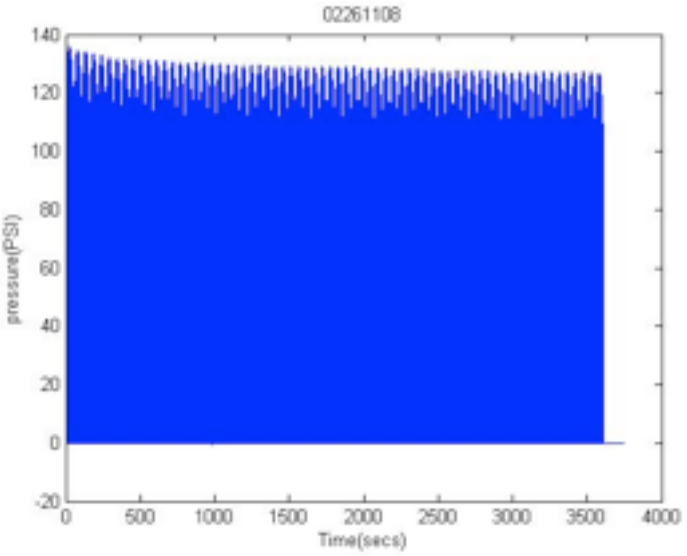

Figure 6a. Pressure data for 1 hour cyclic trial.

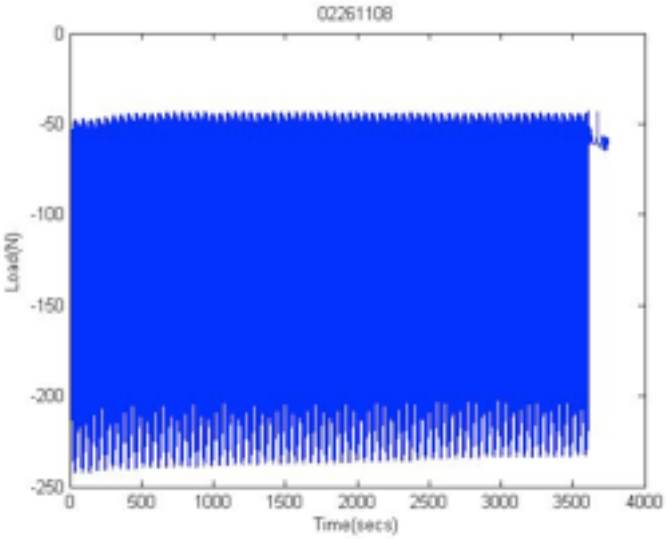

Figure 6b. Load data for 1 hour cyclic trial.

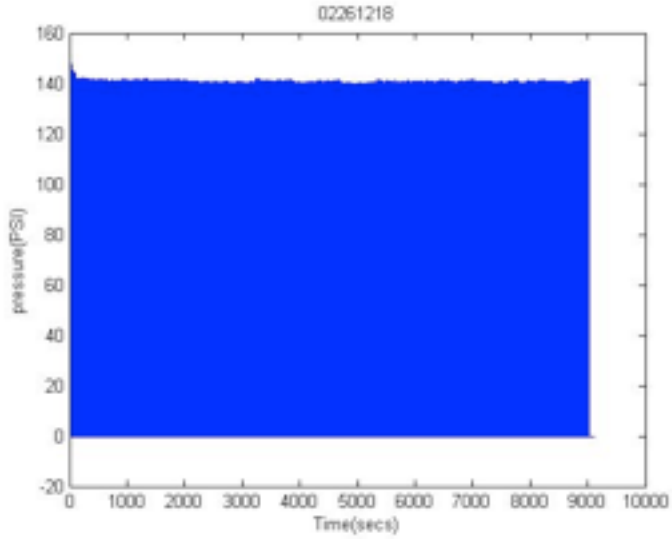

Figure 7a. Pressure data for 1 hour cyclic trial.

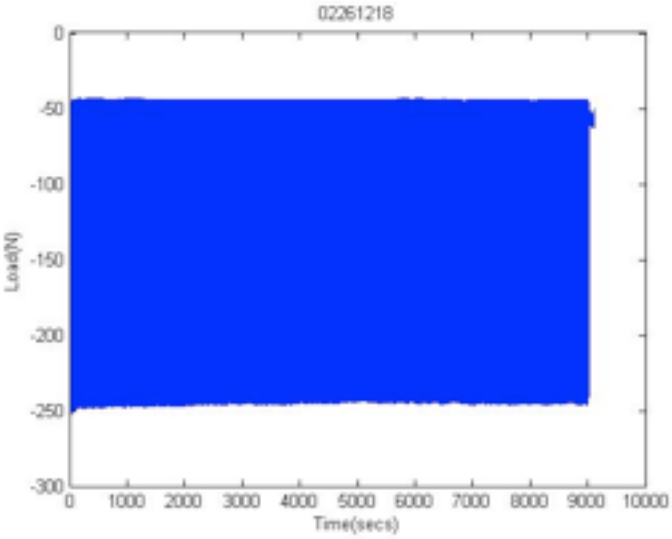

Figure 7b. Load data for 1 hour cyclic trial.

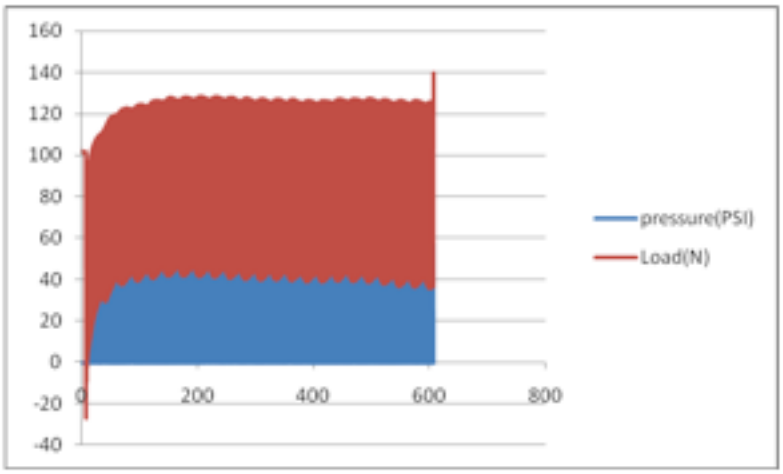

Figure 8a. Pressure and load cycle in a 10 minute cyclic trial.

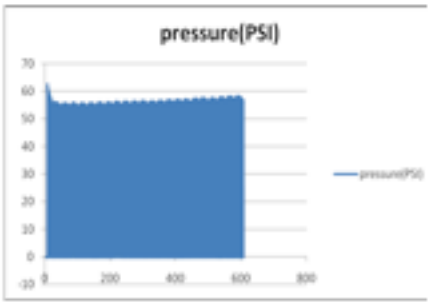

Figure 8b. Pressure data for 10 minute cyclic trial.

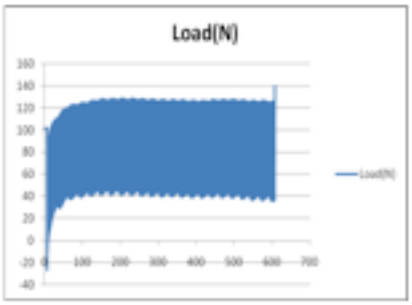

Figure 8c. Load data for 10 minute cyclic trial.

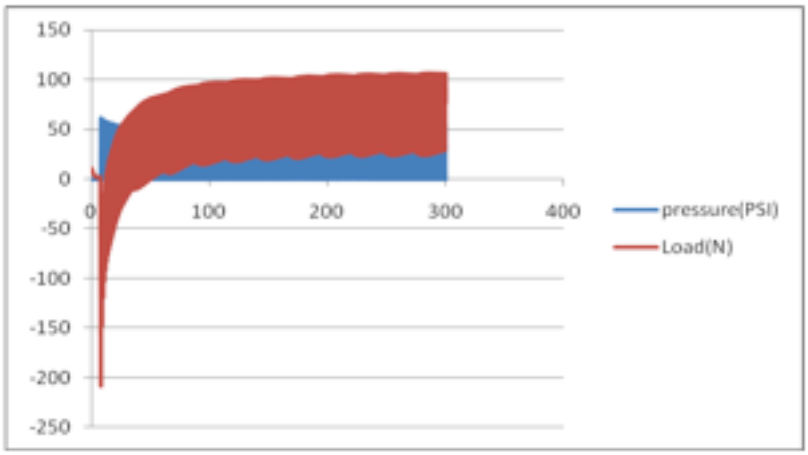

Figure 9a. Pressure and load cycle in a 5 minute cyclic trial.

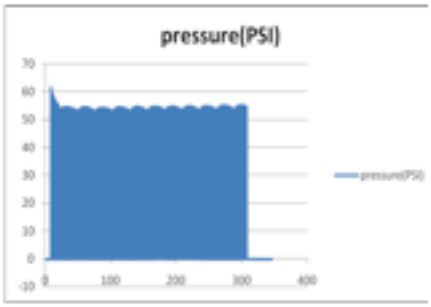

Figure 9b. Pressure data for 5 minute cyclic trial.

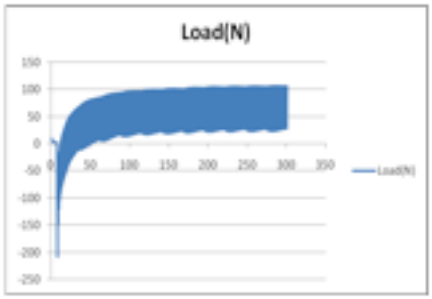

Figure 9c. Load data for 5 minute cyclic trial.

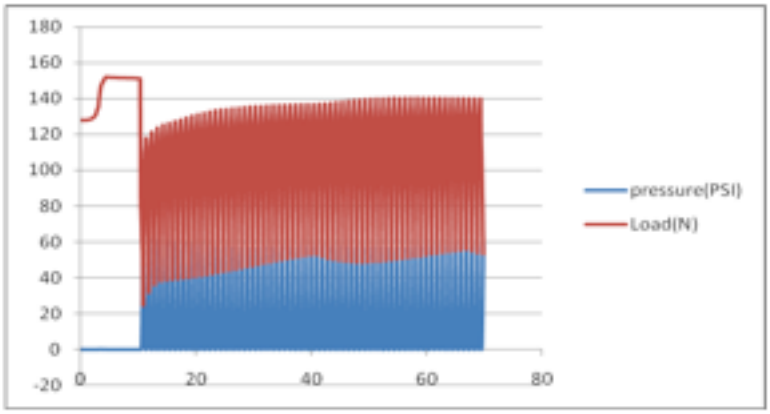

Figure 10a. Pressure and load cycle in a 1 minute cyclic trial.

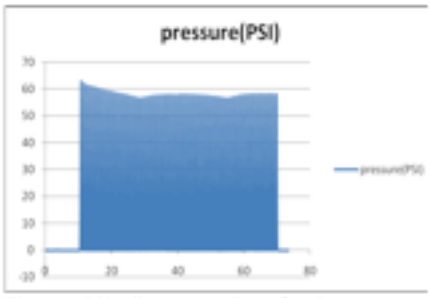

Figure 10b. Pressure data for 1 minute cyclic trial.

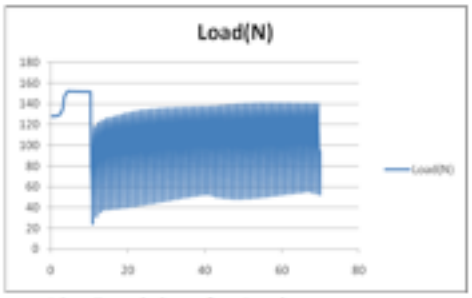

Figure 10c. Load data for 1 minute cyclic trial.

2. In constant pressure cycles, a more considerable change in pressure and load data was observed.

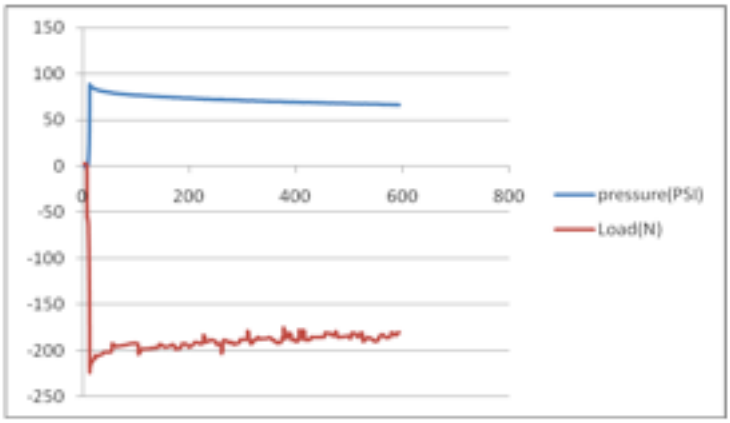

Figure 11a. Pressure and load in a 10 minute trial

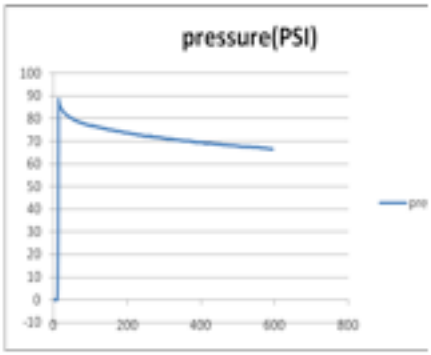

Figure 11b. Pressure data for 10 minute trial.

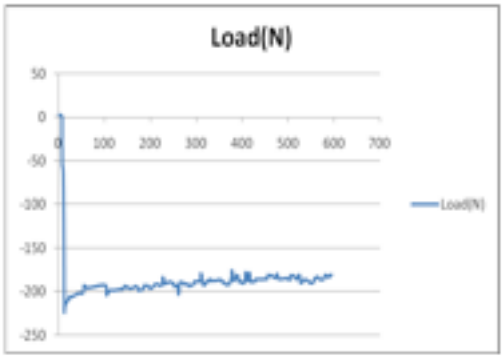

Figure 11c. Load data for 10 minute trial.

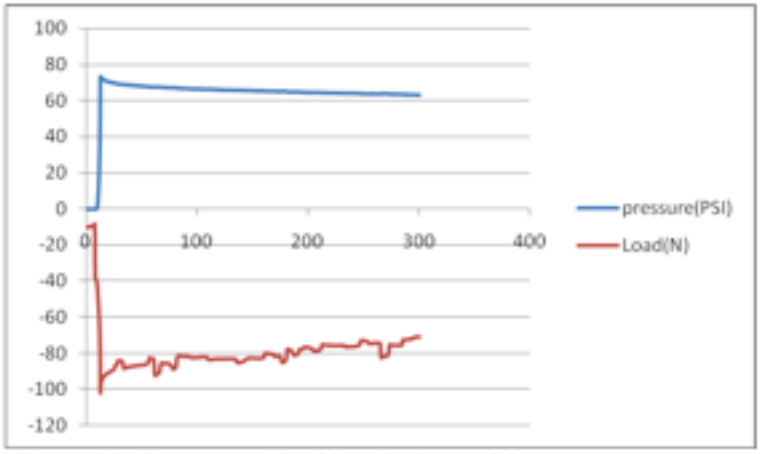

Figure 12a. Pressure and load in a 5 minute trial

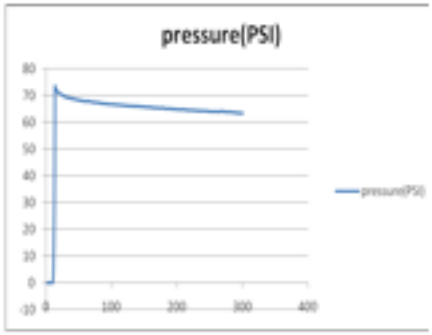

Figure 12b. Pressure data for 5 minute trial.

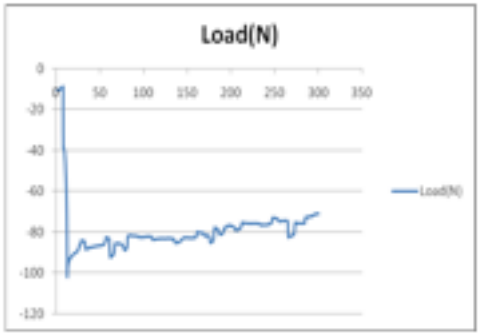

Figure 12c. Load data for 5 minute trial.

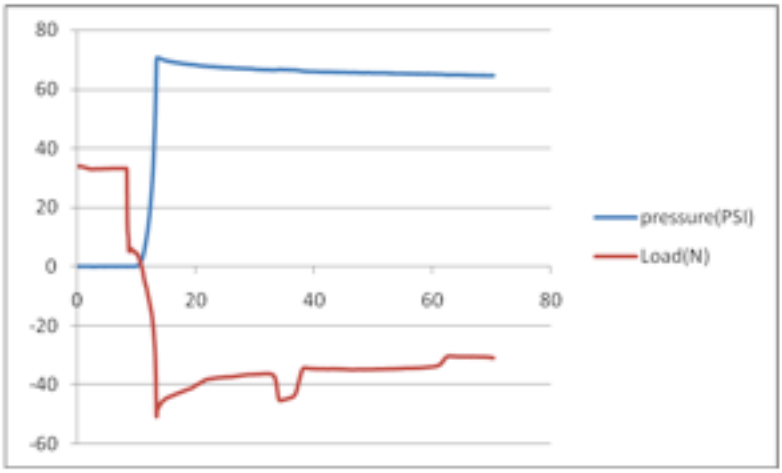

Figure 13a. Pressure and load in a 1 minute trial

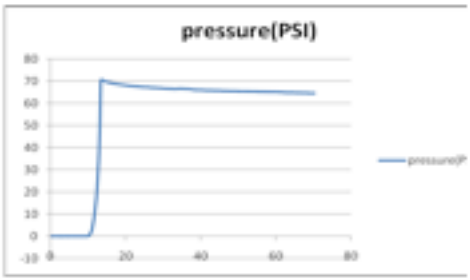

Figure 13b. Pressure data for 1 minute trial.

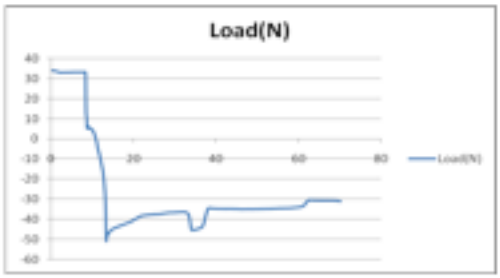

Figure 13c. Load data for 1 minute trial